Atomic defects in topological and correlated twisted van der Waals heterostructures

Jose Lado

Department of Applied Physics, Aalto University, Finland

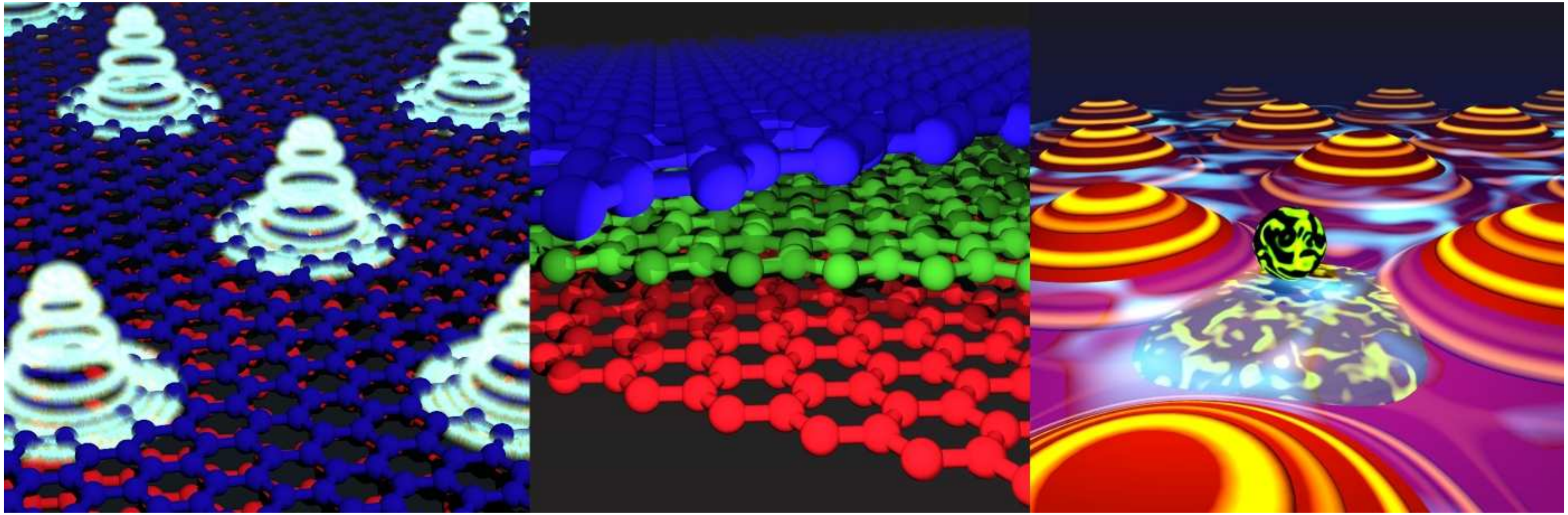

Phys. Rev. B 99, 245118 (2019)
Phys. Rev. Materials 3, 084003 (2019)

Phys. Rev. Research 2, 033357 (2020)

arXiv:2202.11003 (2022)

Condensed matter theory of 2D materials seminar, University of Manchester, UK

June 8th 2022

Building quantum matter with artificial lattices

Atomic lattices	Twisted 2D moire materials	Cold atoms
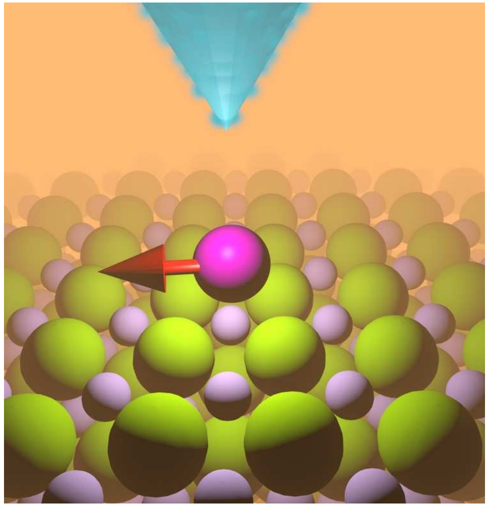	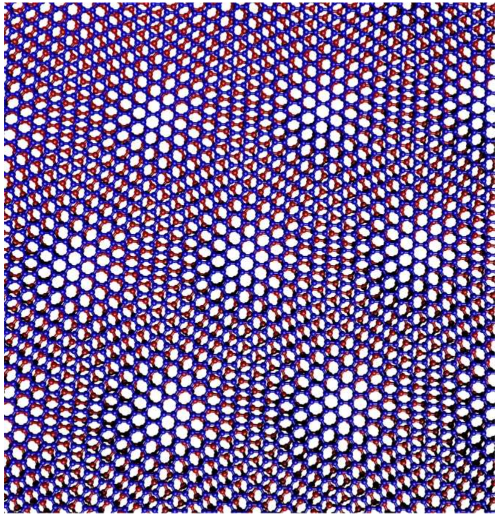	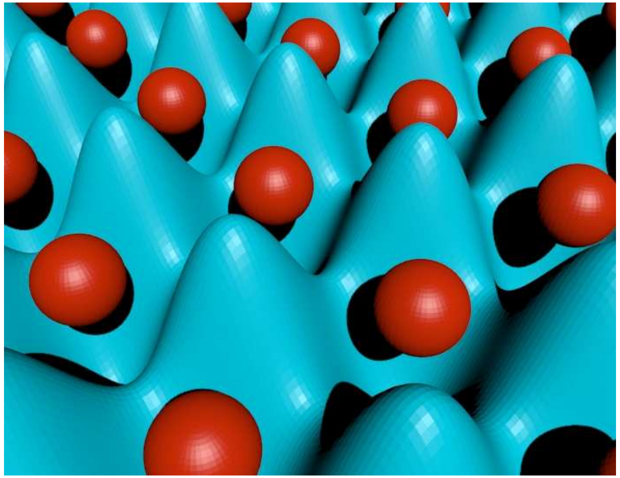
a = 0.5 nm	a = 30 nm	a = 1000 nm
Nature Physics 12 (7), 656 (2016) *Nature Physics 13 (7) 668 (2017)* *Science 335 (6065), 196-199 (2012)*	*Phys. Rev. Lett. 99, 256802 (2007)* *Nature Physics 6, 109–113 (2010)* *PNAS 108 (30) 12233-12237 (2011)* *Nature 556, 80–84 (2018)*	*Nature 545, 462–466 (2017)* *Nature 455, 204–207 (2008)* *Phys. Rev. Lett. 111, 185307 (2013)*

A new universe in each new twisted material

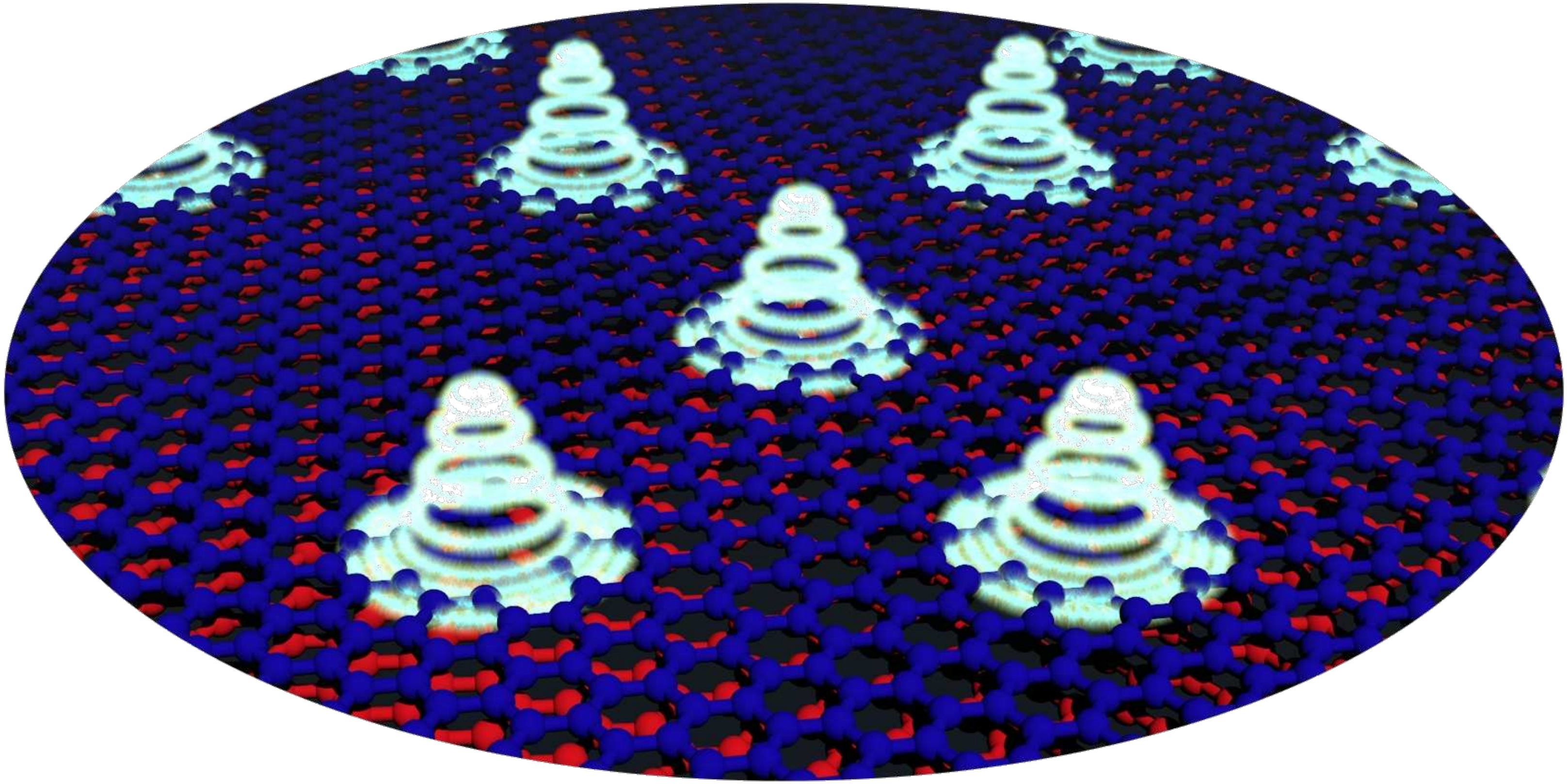

Each twisted material is a new universe for electrons, with laws that change from twist to twist

The two-dimensional materials world

Semimetal

Graphene

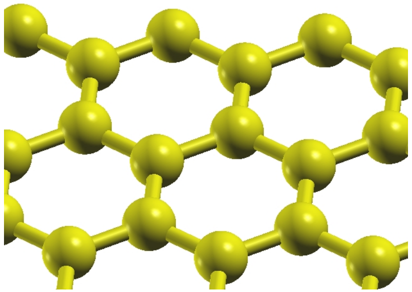

Insulator

BN

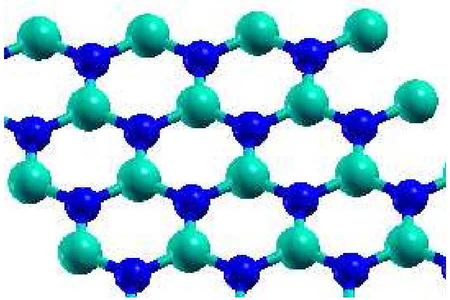

Superconductor

$NbSe_2$

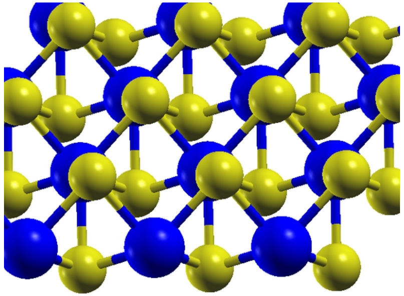

Ferroelectric

SnTe

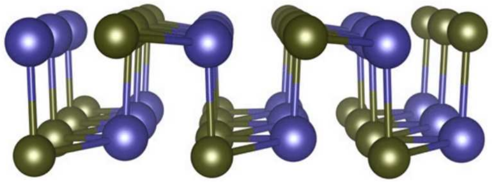

Semiconductor

WSe_2

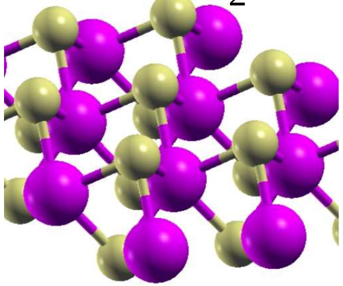

Ferromagnet

CrI_3

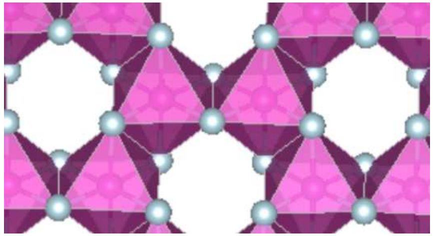

Quantum spin Hall insulator

WTe_2

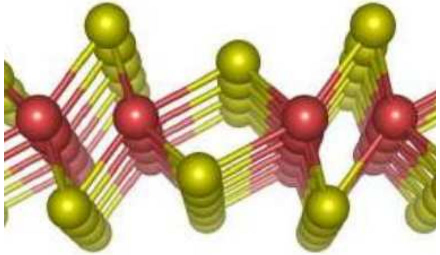

Multiferroic

NiI_2

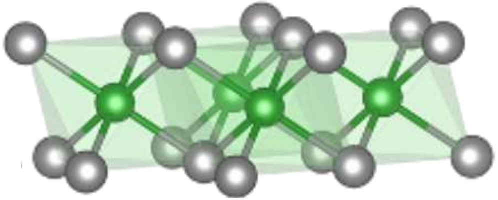

The flexibility of two-dimensional materials

They can be stacked

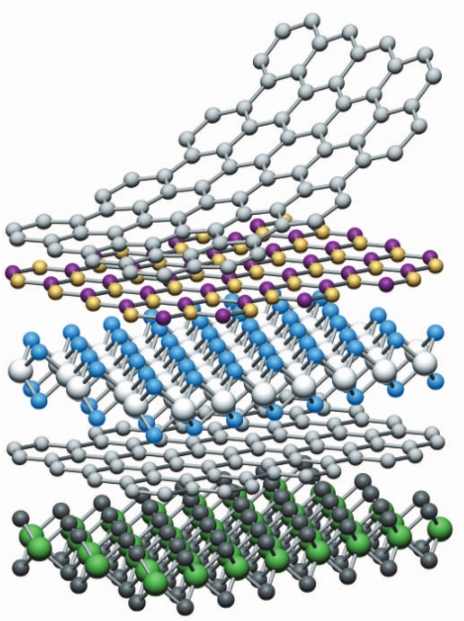

Nature 499.7459 419. (2013)

They can be rotated

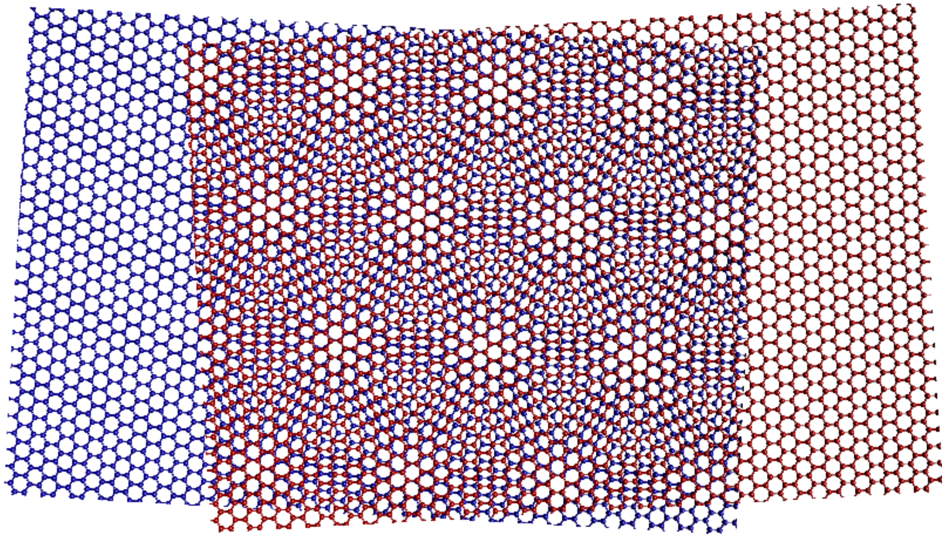

Science 361.6403 690-693. (2018)

These are unique features of two-dimensional materials

Moire in twisted bilayer graphene

Upper graphene layer

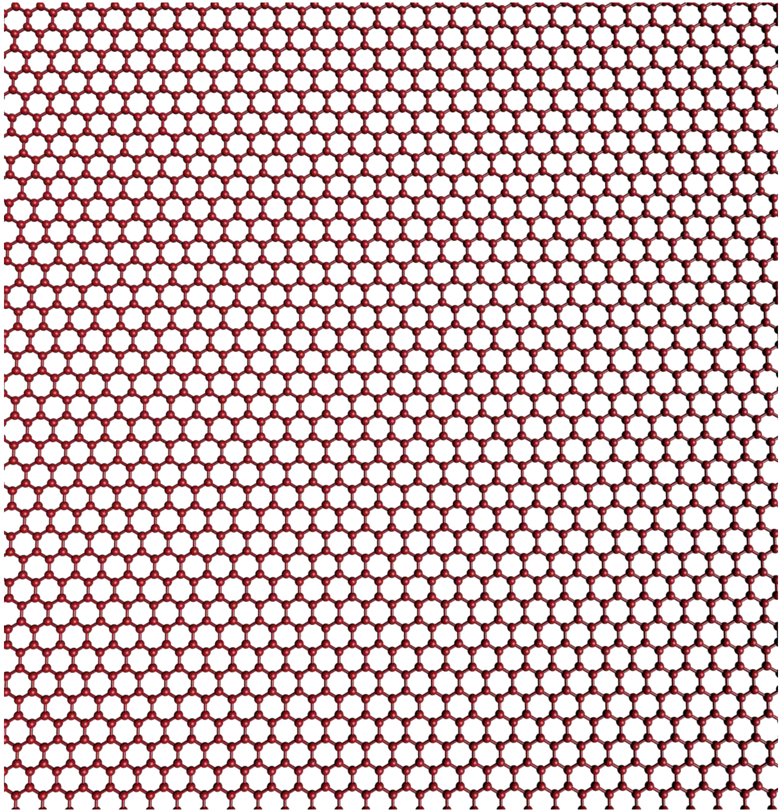

Lower graphene layer

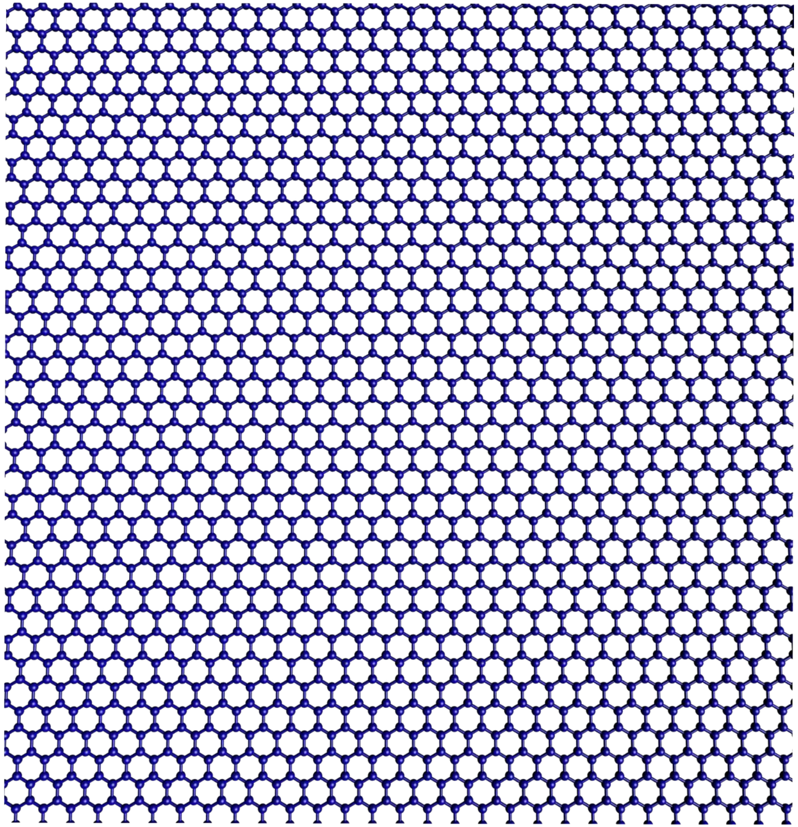

Moire in twisted bilayer graphene

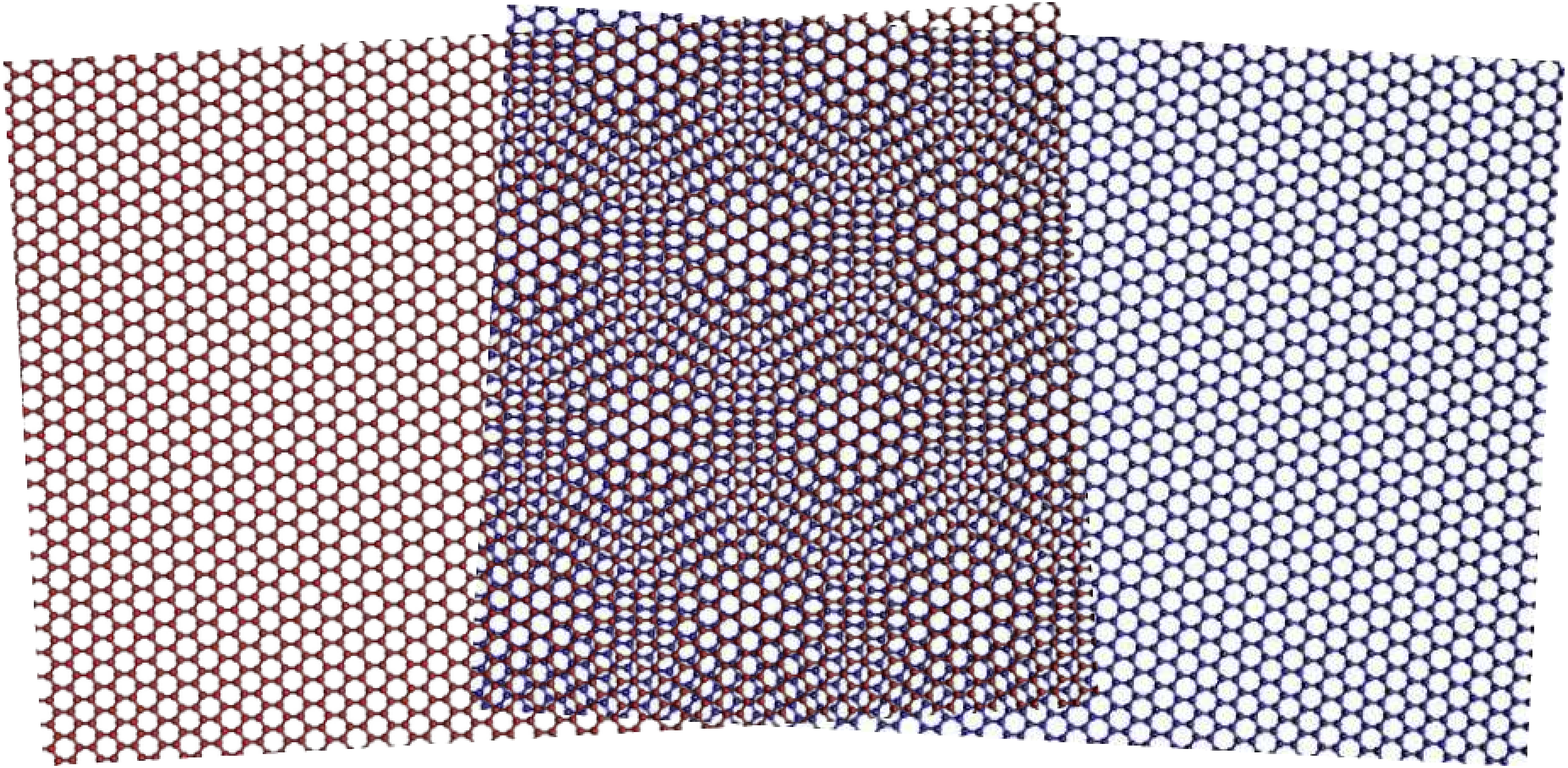

Moire in twisted bilayer graphene

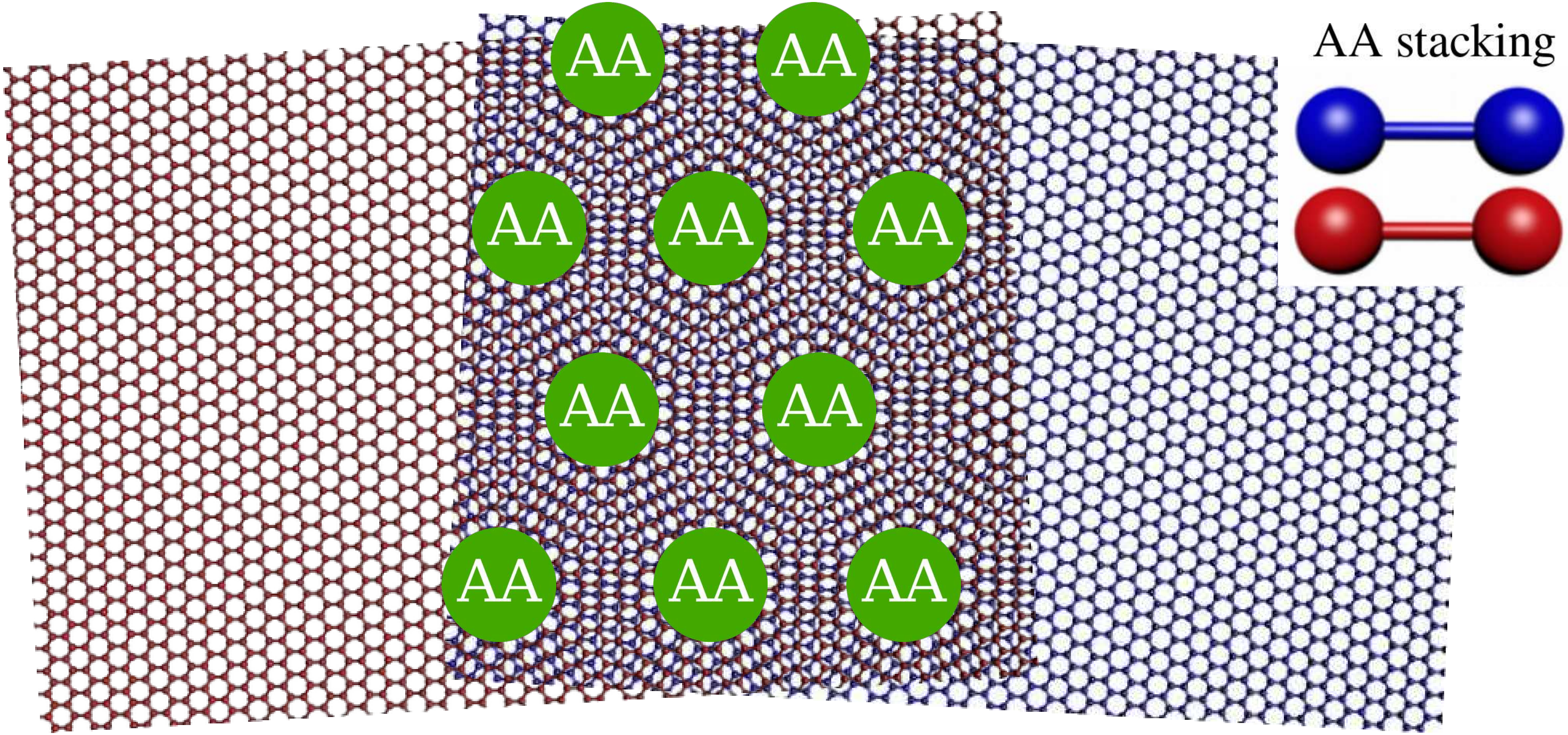

Moire in twisted bilayer graphene

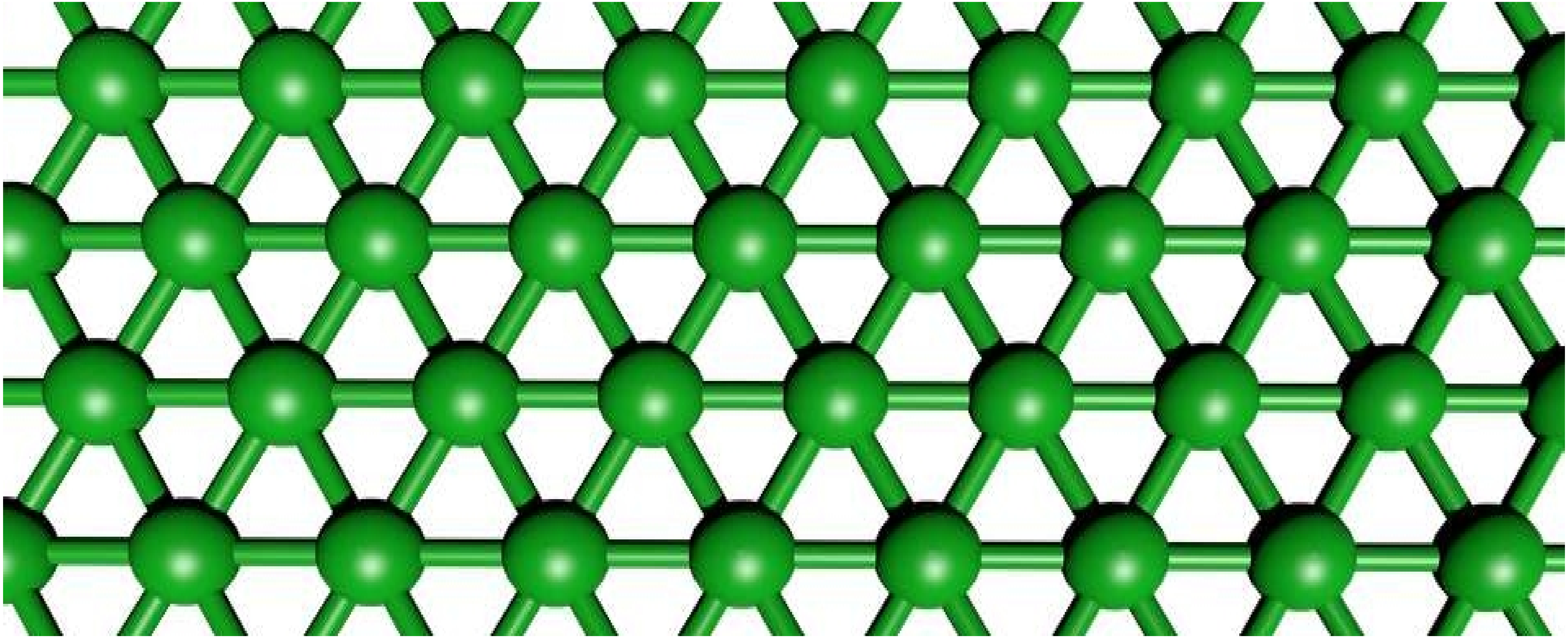

One material, a zoo of electronic phases

Twisted bilayer graphene

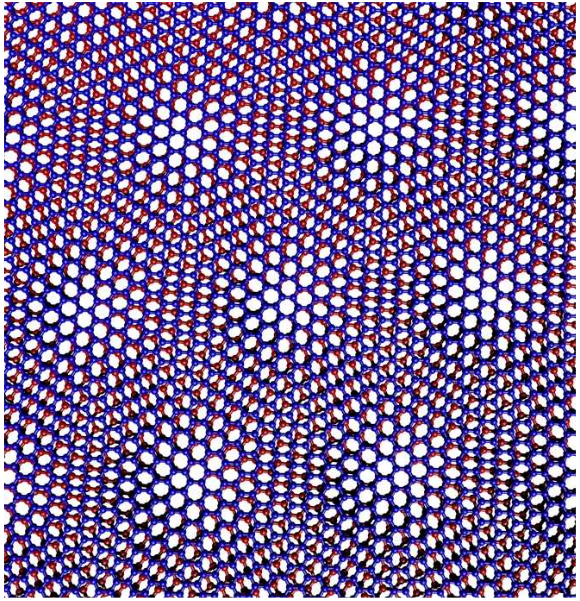

Superconductivity

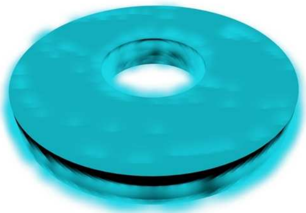

Nature 556, 43–50 (2018)

Topological networks

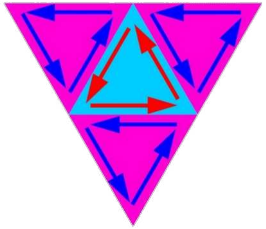

Nano Lett. 18, 11, 6725-6730 (2018)

Chern insulators

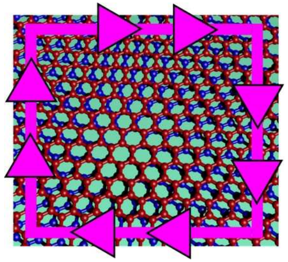

Science 365, 605-608 (2019)

Correlated insulators

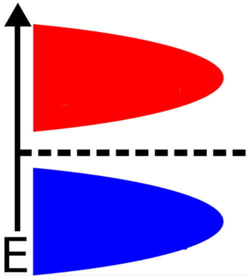

Nature 556, 80–84 (2018)

Quasicrystalline physics

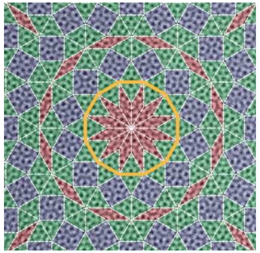

Science 361, 782-786 (2018)

Fractional Chern insulators

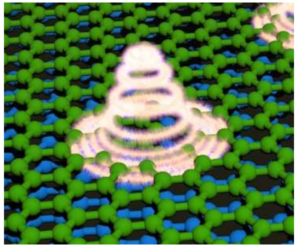

Nature 600, 439–443 (2021)

Twisted graphene multilayers provide a powerful platform for emergent phenomena

Unique properties of moire systems

In addition to all the features of conventional materials, twisted multilayers feature (among others)

Control via twist engineering

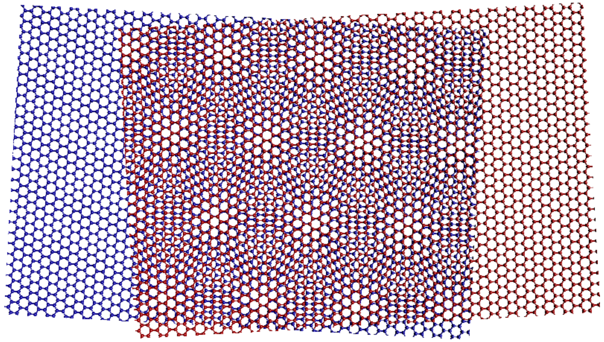

Phys. Rev. B 82, 121407(R) (2010)
PNAS 108 (30) 12233-12237 (2011)
Nature Reviews Materials 6, 201–206 (2021)

Strong electrostatic band distortions

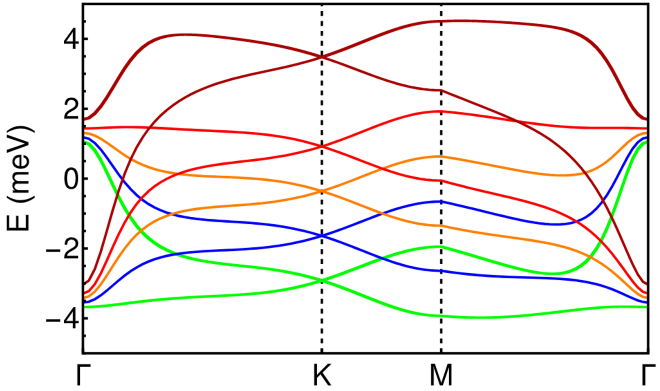

PNAS 115 (52), 13174-13179 (2018)
Physical Review B 99 (20), 205134 (2019)

Defects in two different length scales

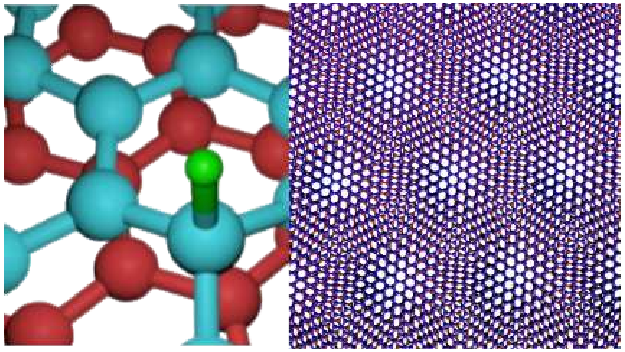

Nature 581, 47–52 (2020)
Today’s plan

Moire and impurities

Two length scales in moire systems

The original atomic scale

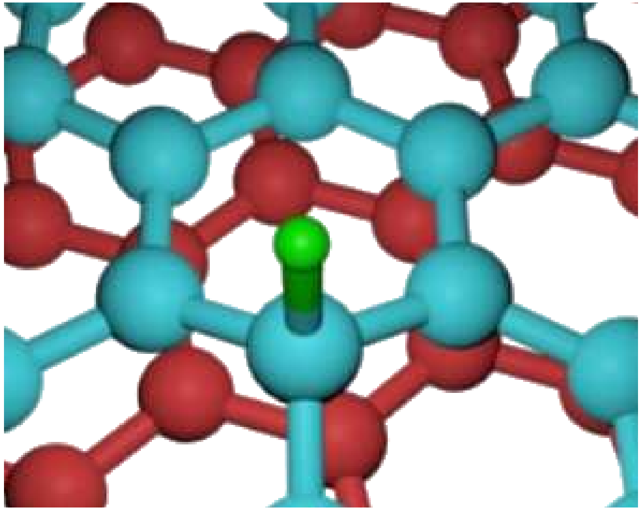

The emergent moire scale

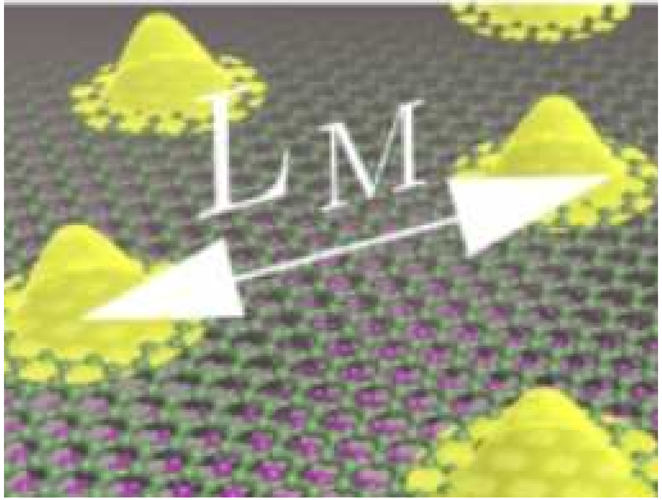

The coexistence of these two different scales is unique to moire systems

How do atomic impurities impact the physics emerging from much bigger length scales?

Today’s plan

Impurities in twisted graphene bilayers

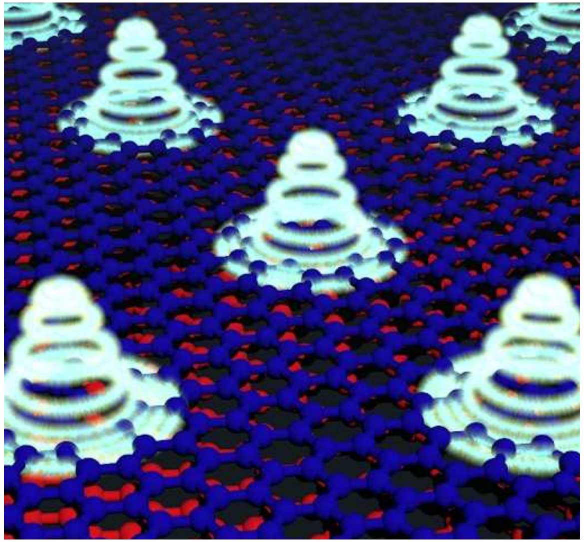

Phys. Rev. B 99, 245118 (2019)
Phys. Rev. Materials 3, 084003 (2019)

Impurities in twisted graphene trilayers

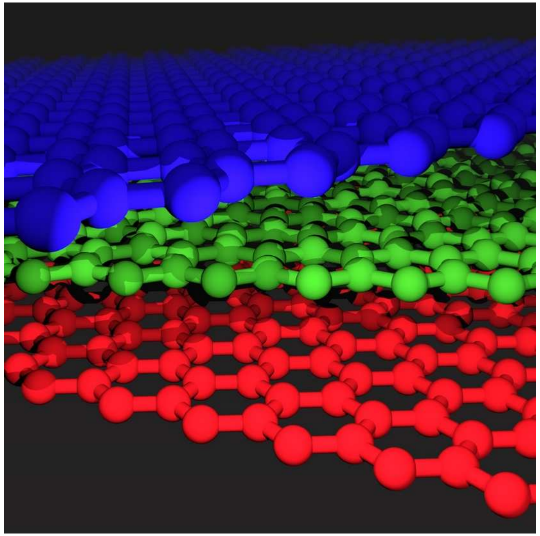

Phys. Rev. Research 2, 033357 (2020)

Impurities in twisted moire topological superconductors

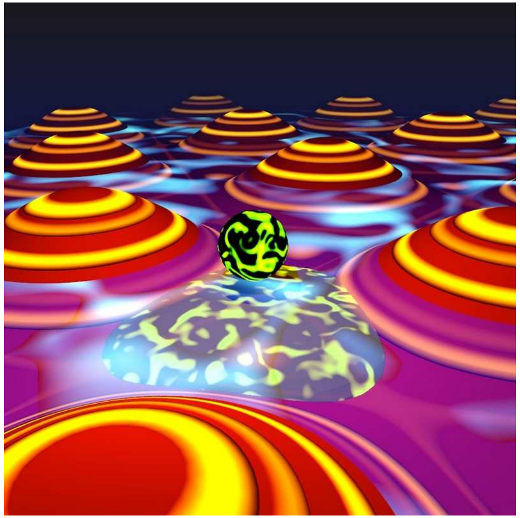

arXiv:2202.11003 (2022)

Behind the scenes

Impurities in twisted graphene bilayers

Aline Ramires

Phys. Rev. B 99, 245118 (2019)

Impurities in twisted graphene trilayers

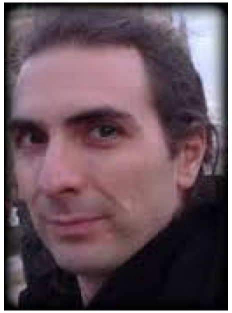

Alejandro Lopez Bezanilla

Phys. Rev. Research 2, 033357 (2020)
Phys. Rev. Materials 3, 084003 (2019)

Impurities in twisted moire topological superconductors

Maryam Khosravian

arXiv:2202.11003 (2022)

Impurities in twisted bilayer graphene

Twisted graphene bilayers

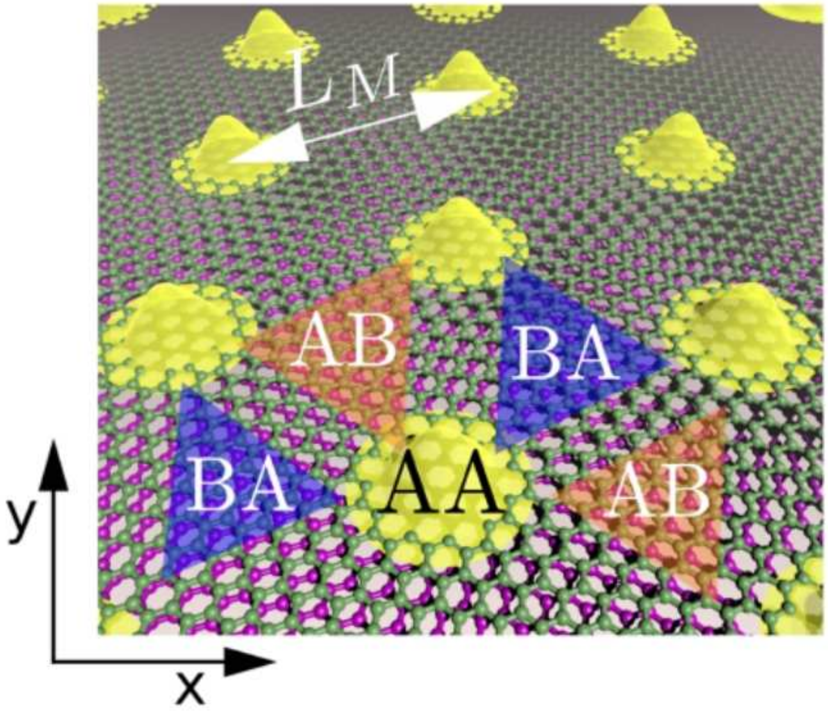

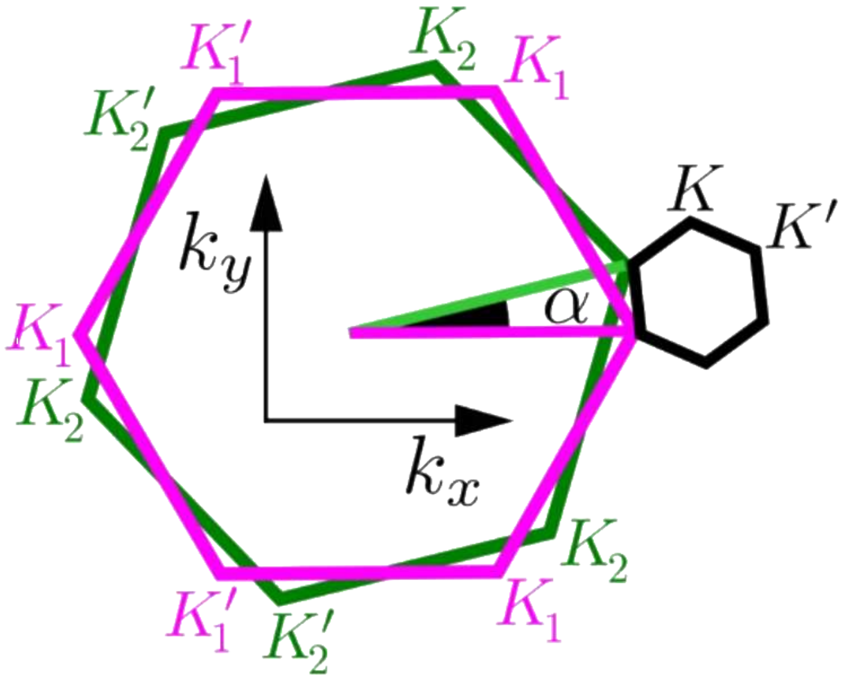

Impact of single impurities in the twisted bilayer electronic structure

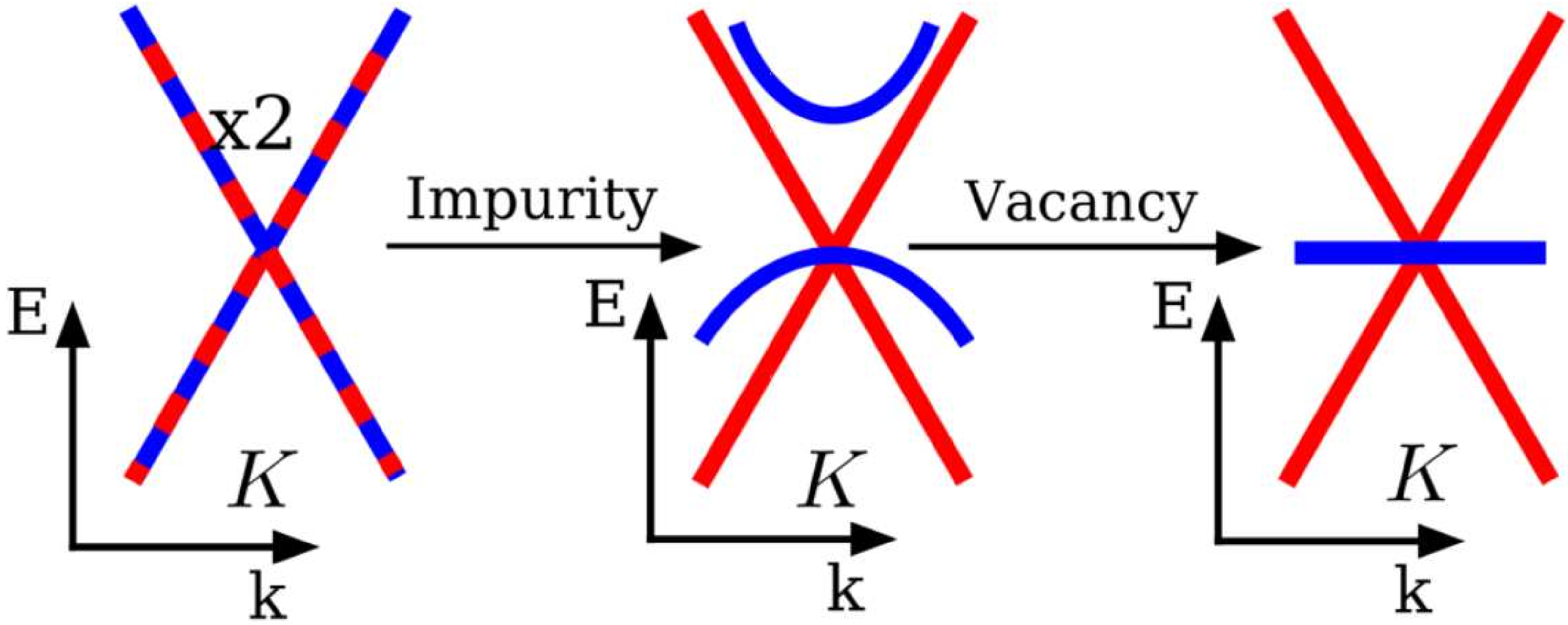

Single impurities give rise to a triple point crossing in the electronic structure

Model for impurities in twisted multilayers

Full Hamiltonian

$$\mathcal{H} = \mathcal{H}_0 + \mathcal{W}$$

Pristine twisted bilayer graphene

$$\mathcal{H}_0 = t \sum_{\langle i,j \rangle} c_i^\dagger c_j + \sum_{i,j} \bar{t}_\perp(\mathbf{r}_i, \mathbf{r}_j) c_i^\dagger c_j$$

Intra-layer hopping

Inter-layer hopping

Local impurity

$$\mathcal{W} = w c_n^\dagger c_n$$

The limit of infinite potential corresponds to removing a site

$$w \rightarrow \infty$$

The strong impurity limit

Adsorbed hydrogen in TBG

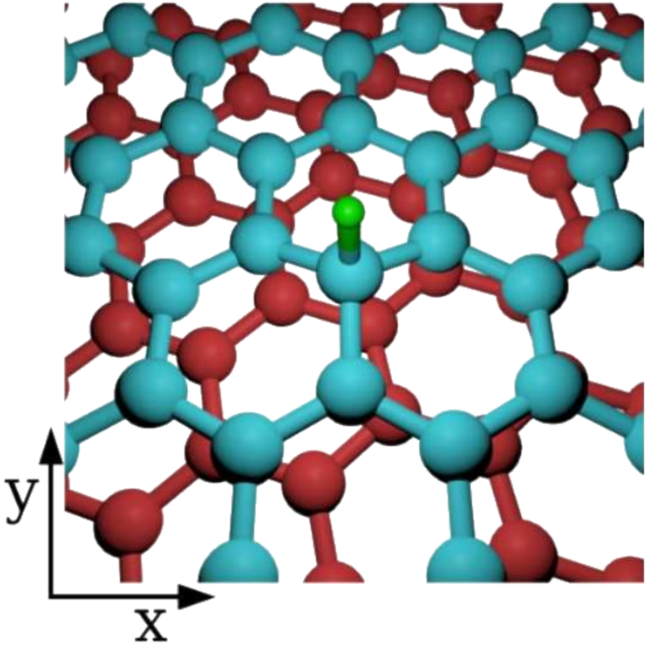

Effective tight binding model

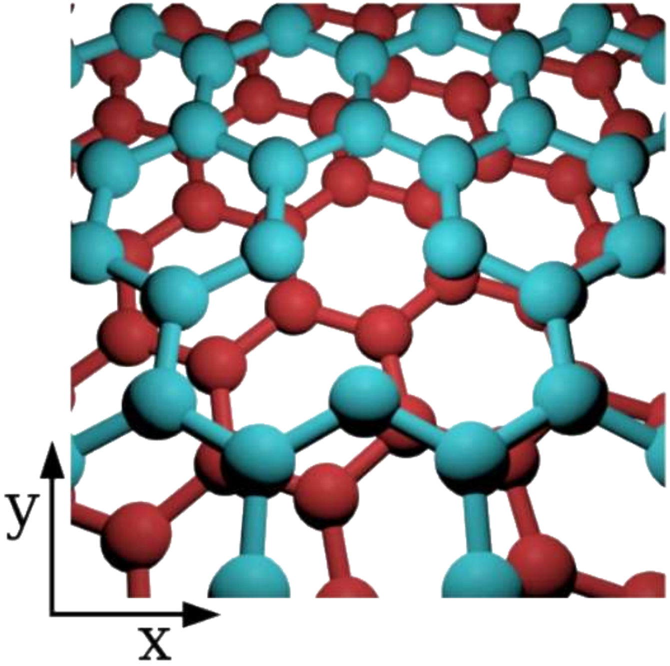

Hydrogen adsorption effectively gives rise to a vacancy in the low energy model

DFT versus tight binding

Density functional theory

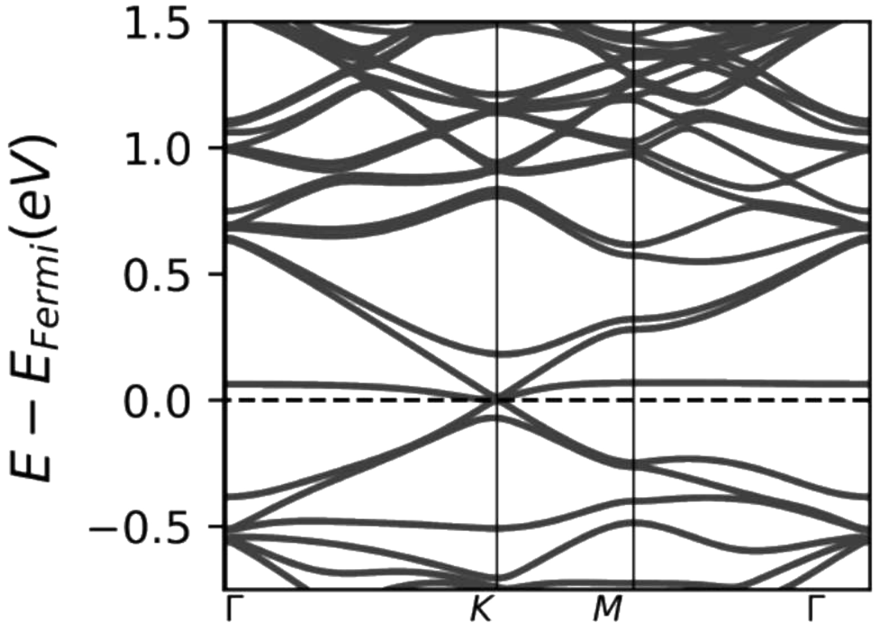

Tight binding

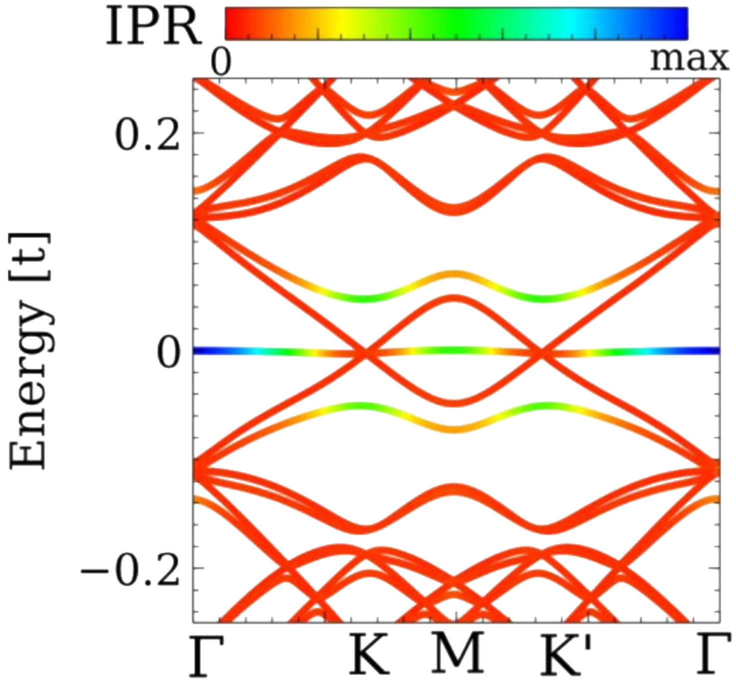

DFT and tight binding give rise to comparable electronic structures

Impact of a single weak defect

Band structure

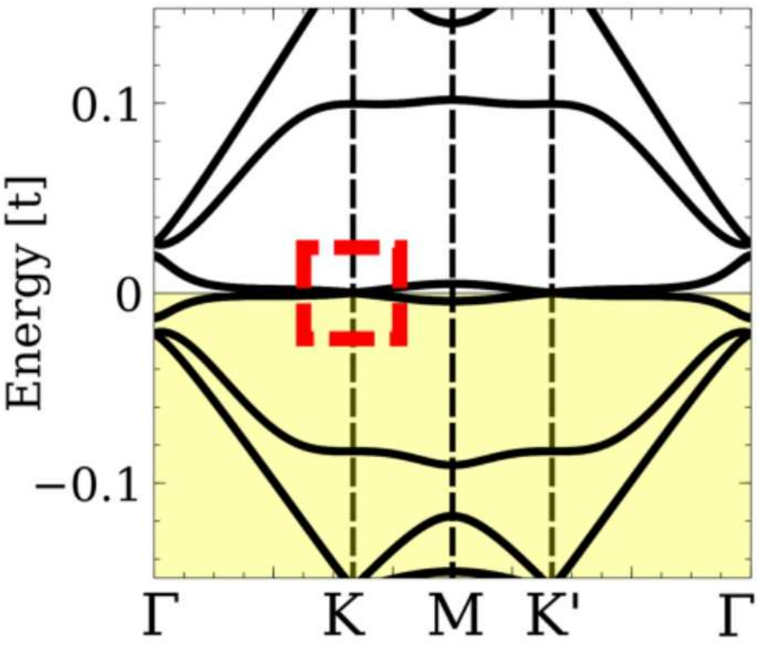

Valley expectation value

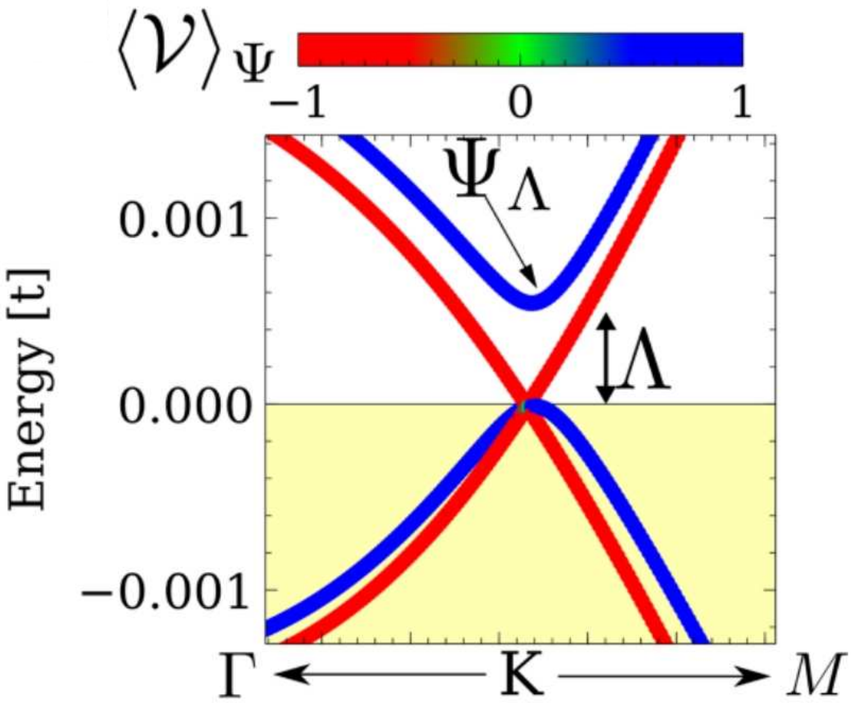

A weak impurity generates a triple band crossing at the Dirac point

Position-dependent valley mixing

Gap opening depending on the location

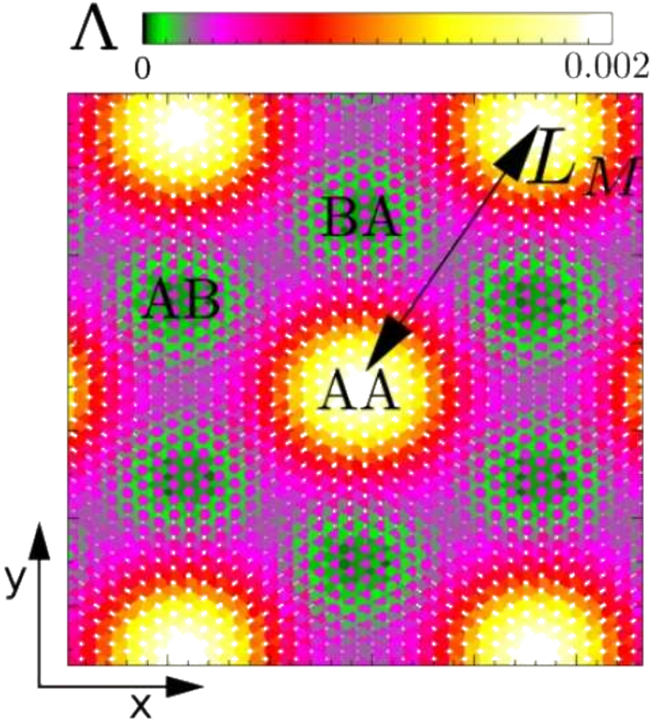

Valley polarization depending on the location

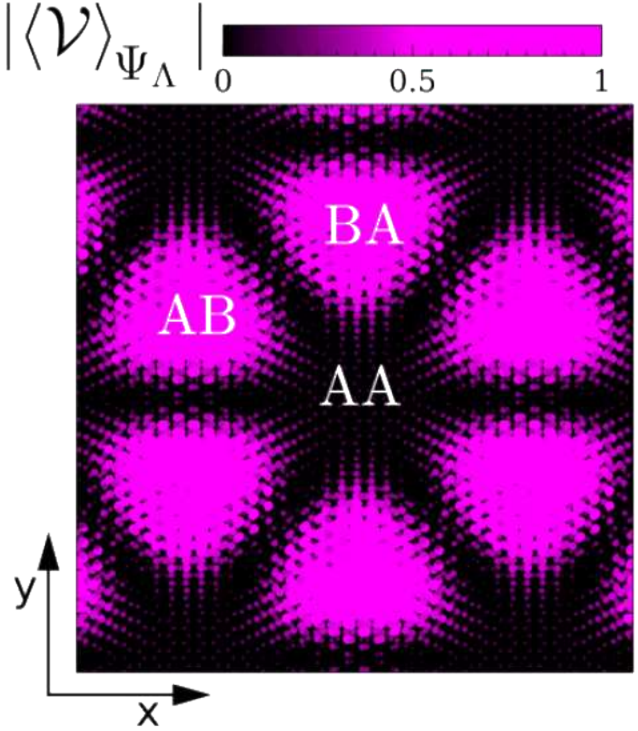

The location of the impurities determines the strength of the valley mixing

Low energy states, pristine bilayer

Band structure

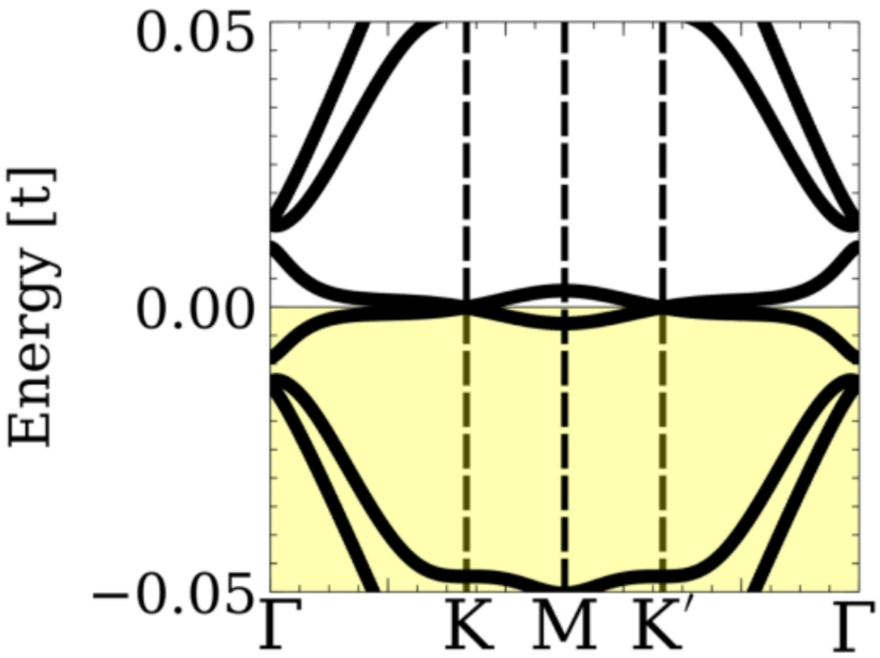

Spatial distribution of the low energy states

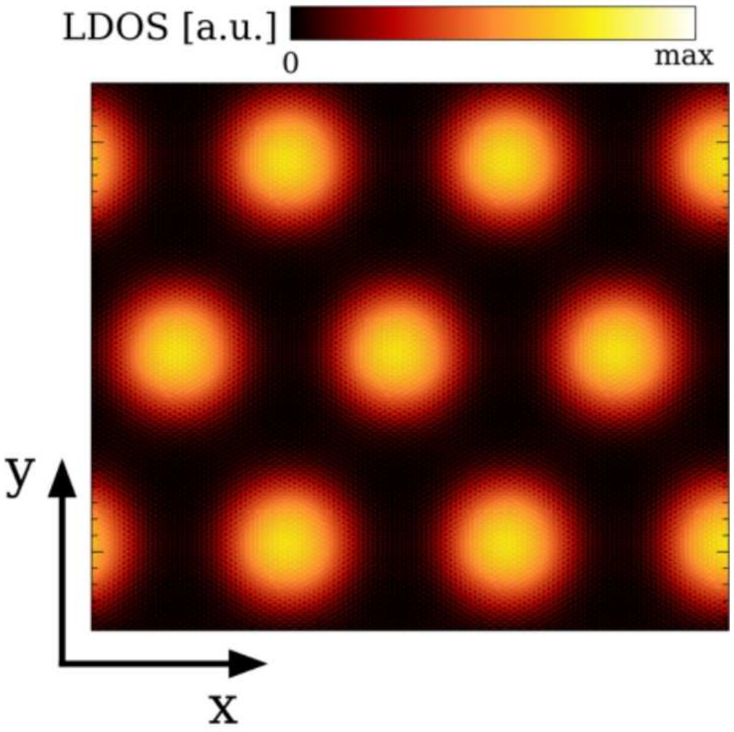

The nearly flat bands create an emergent triangular superlattice

Low energy states, strong single defect

Band structure

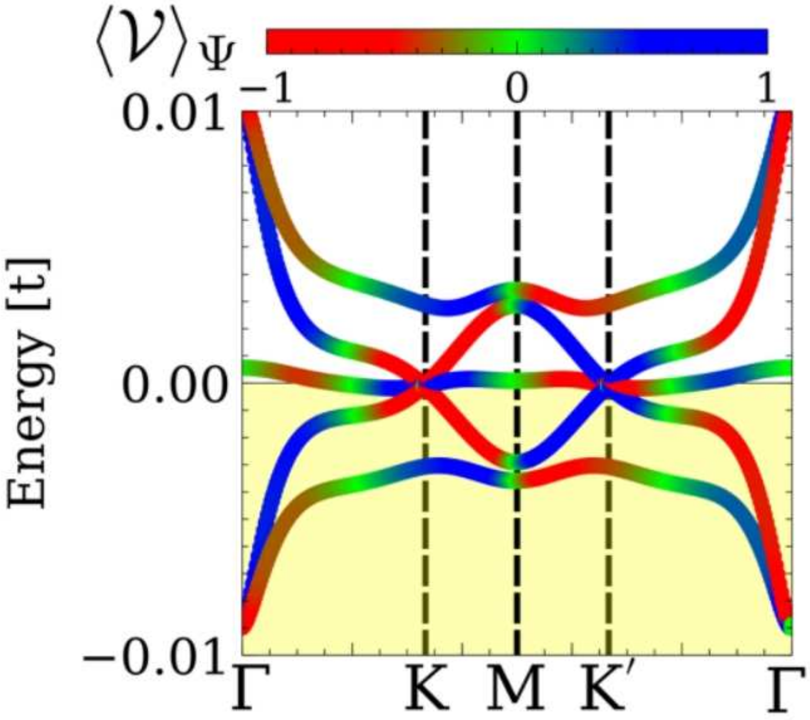

Spatial distribution of the low energy states

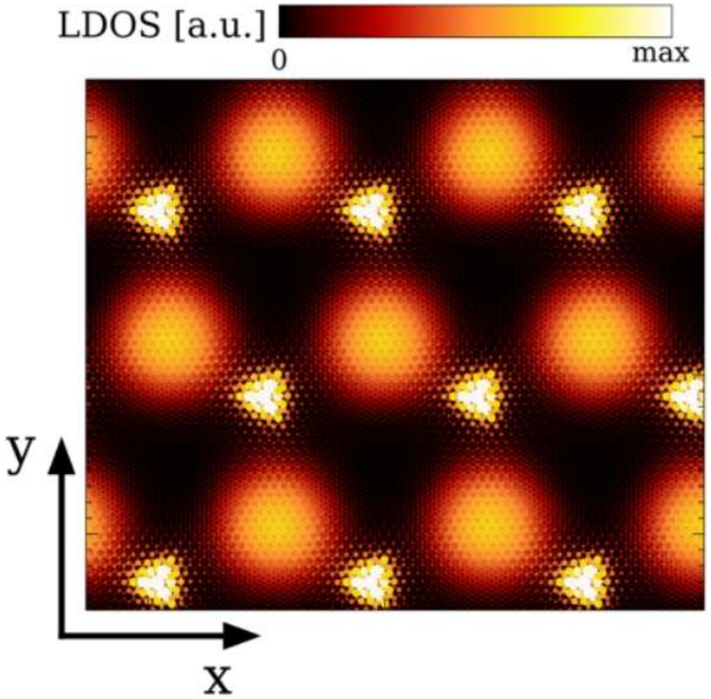

The nearly flat bands coexist with a localized vacancy state

Low energy states, strong single defect in a 4x4 supercell

Band structure

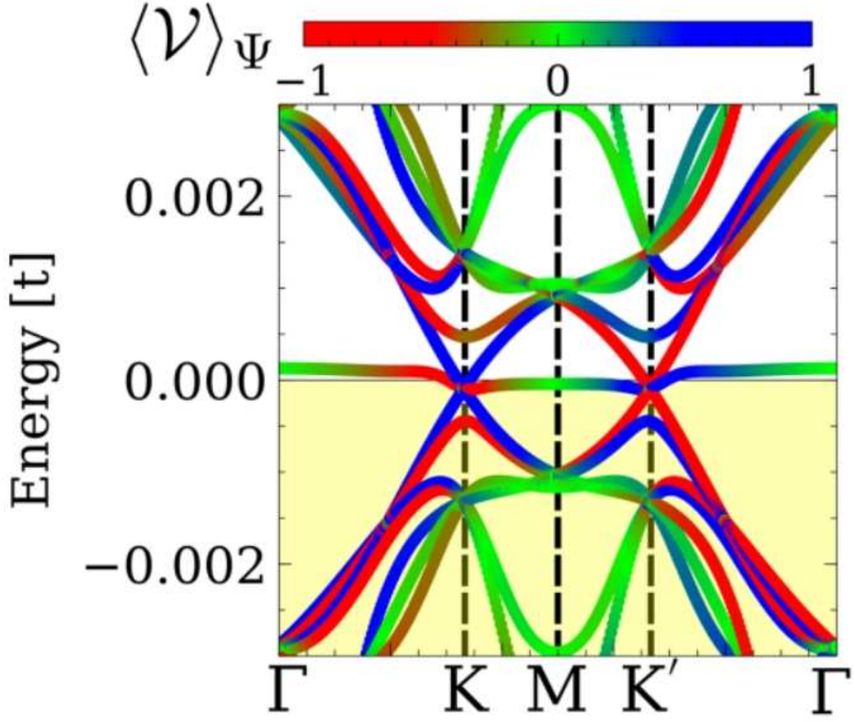

Spatial distribution of the low energy states

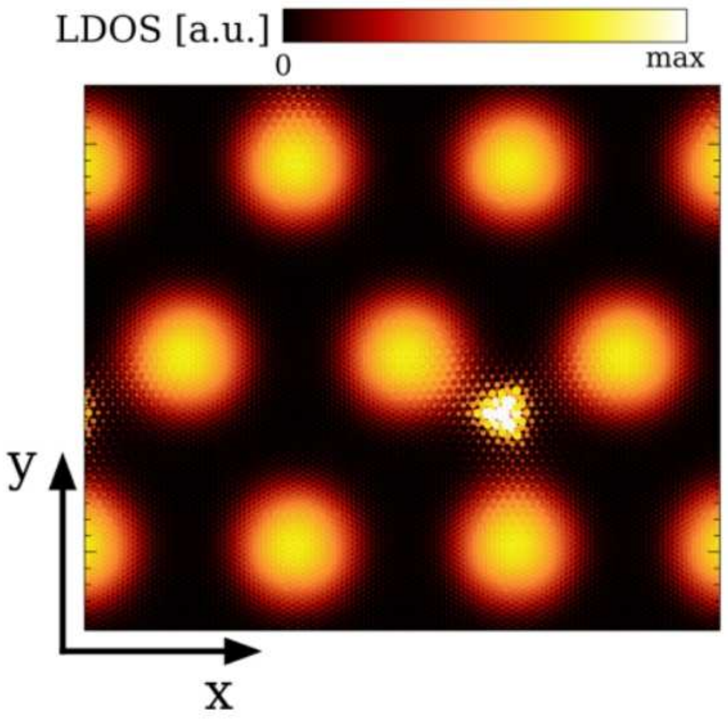

The nearly flat bands coexist with a localized vacancy state

Including interactions in a minimal way

We will include interactions with a minimal Hubbard repulsion

$$H_U = \sum_i U c^\dagger_{i,\uparrow} c_{i,\uparrow} c^\dagger_{i,\downarrow} c_{i,\downarrow} = \sum_i U n_{i,\uparrow} n_{i,\downarrow}$$

Solved at the mean-field level

$$H_U^{\mathrm{MF}} = \sum_i U [\langle n_{i,\uparrow} \rangle n_{i,\downarrow} + \langle n_{i,\downarrow} \rangle n_{i,\uparrow} - \langle n_{i,\uparrow} \rangle \langle n_{i,\downarrow} \rangle]$$

Let us see the impact on the low energy states

Impact of interactions, pristine system

Band structure

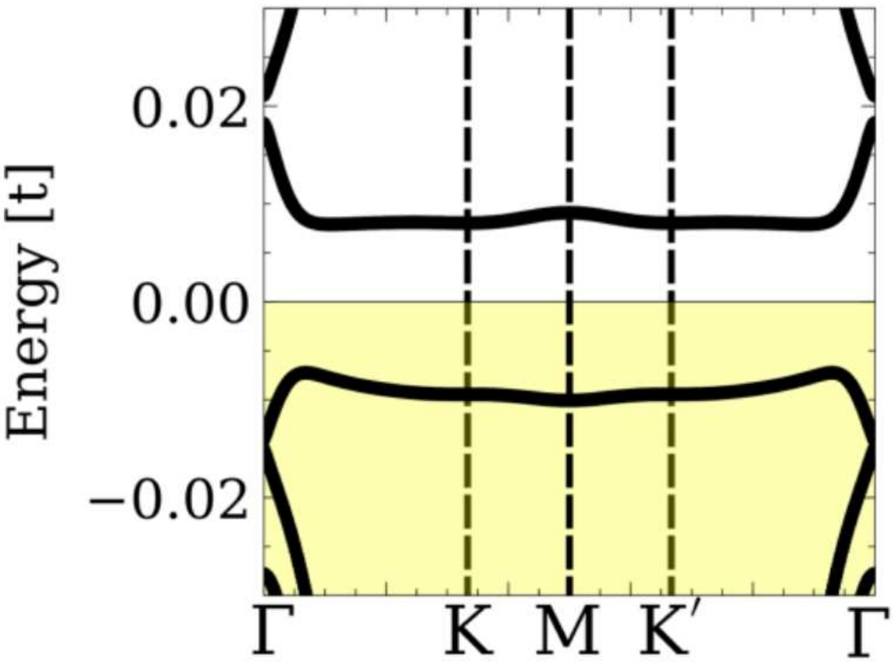

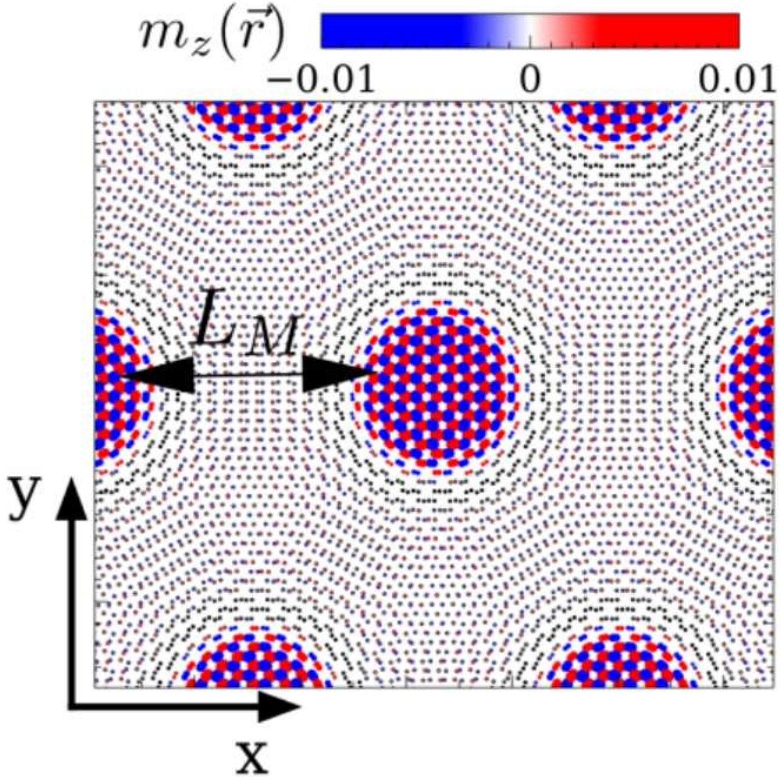

Gap opening at charge neutrality

Impact of interactions, single vacancy at charge neutrality

Band structure

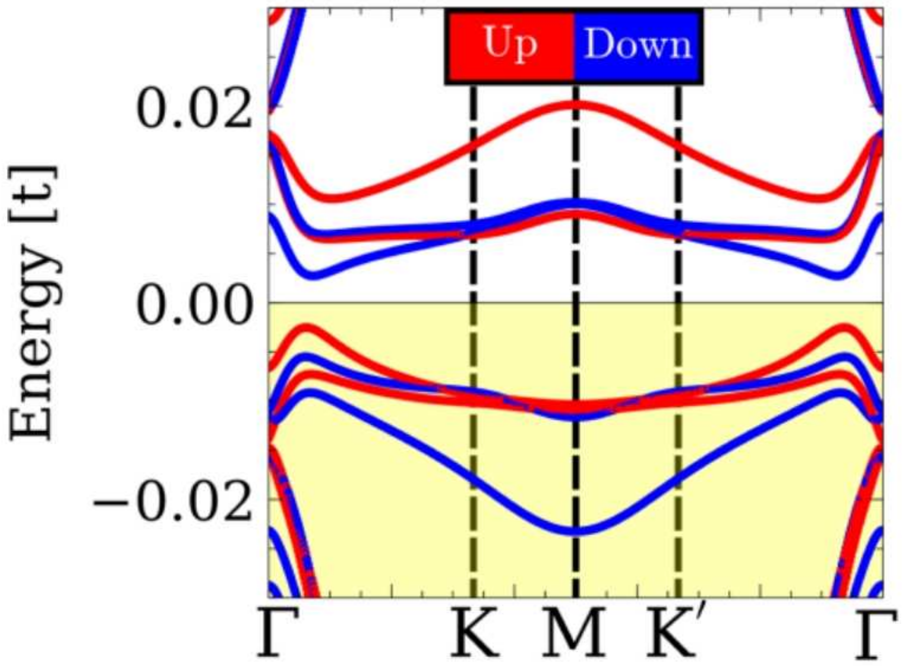

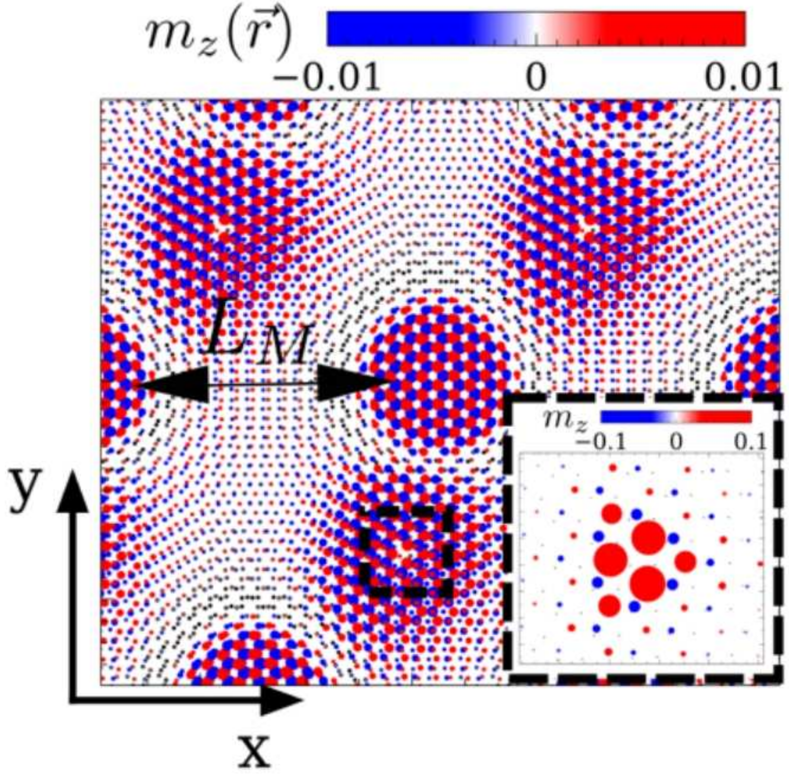

Interaction-driven symmetry breaking in the impurity and flat bands coexists

Impact of interactions, single vacancy at 4e per moire unit cell

Band structure

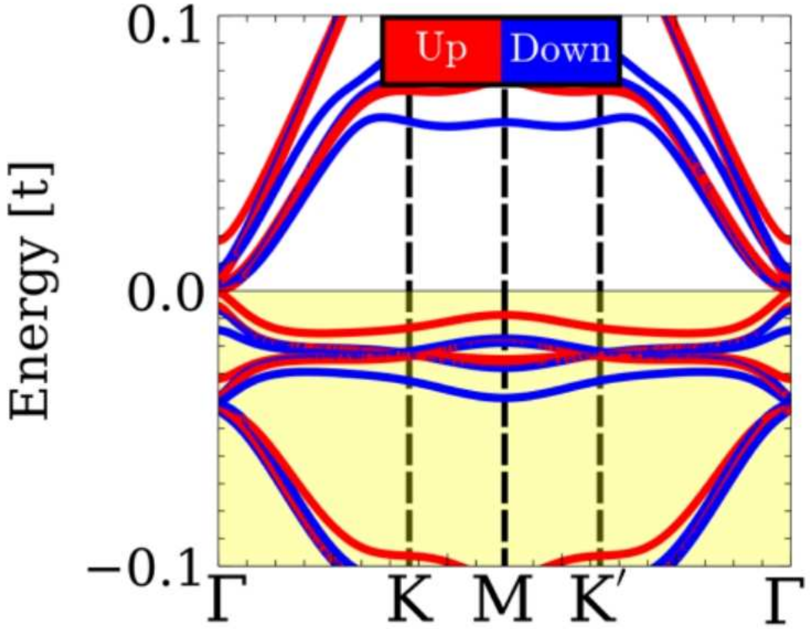

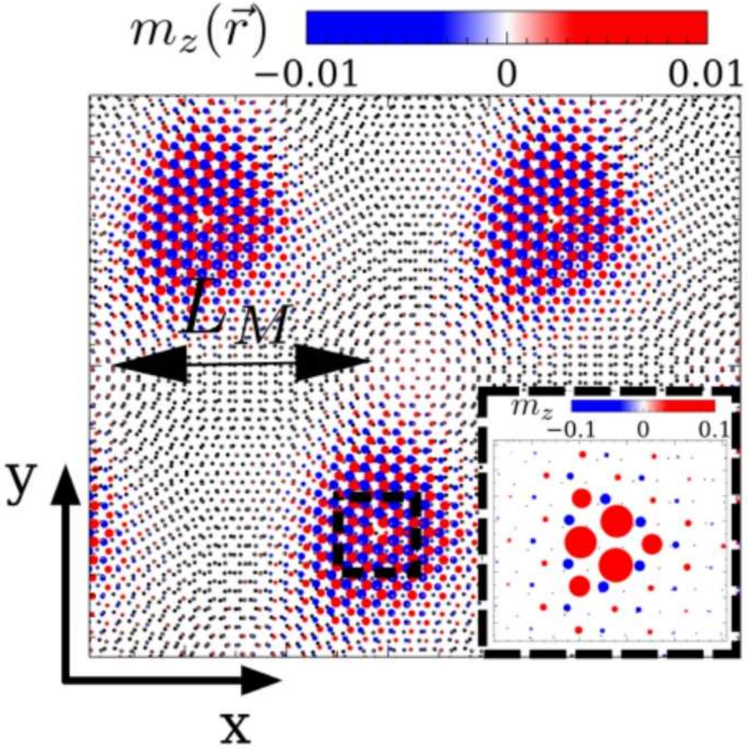

The vacancy magnetism survives full filling of the original twisted bilayer flat bands

Interplay between impurity magnetism and twisted bilayer superconductivity

The impurity induced moment survives doping of the flat bands

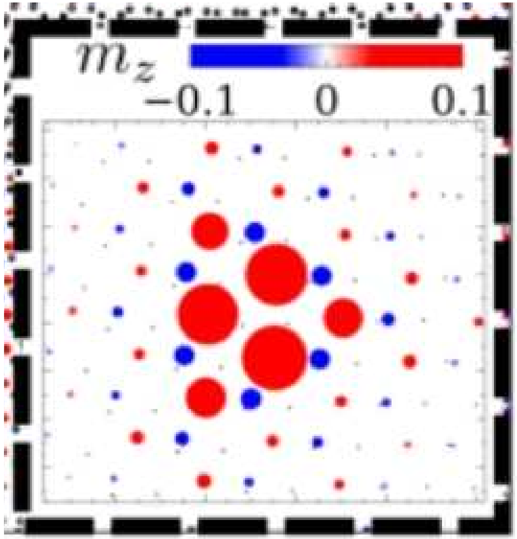

What happens when its magnetism coexists with the twisted bilayer superconducting state?

We will now include a superconducting state

$$H_{SC} = \sum_i \Delta_i [c_{i,\uparrow} c_{i,\downarrow} + c^\dagger_{i,\downarrow} c^\dagger_{i,\uparrow}]$$

Working in the regime of (close to) 2 holes per moire unit cell

Electronic structure
without including interactions

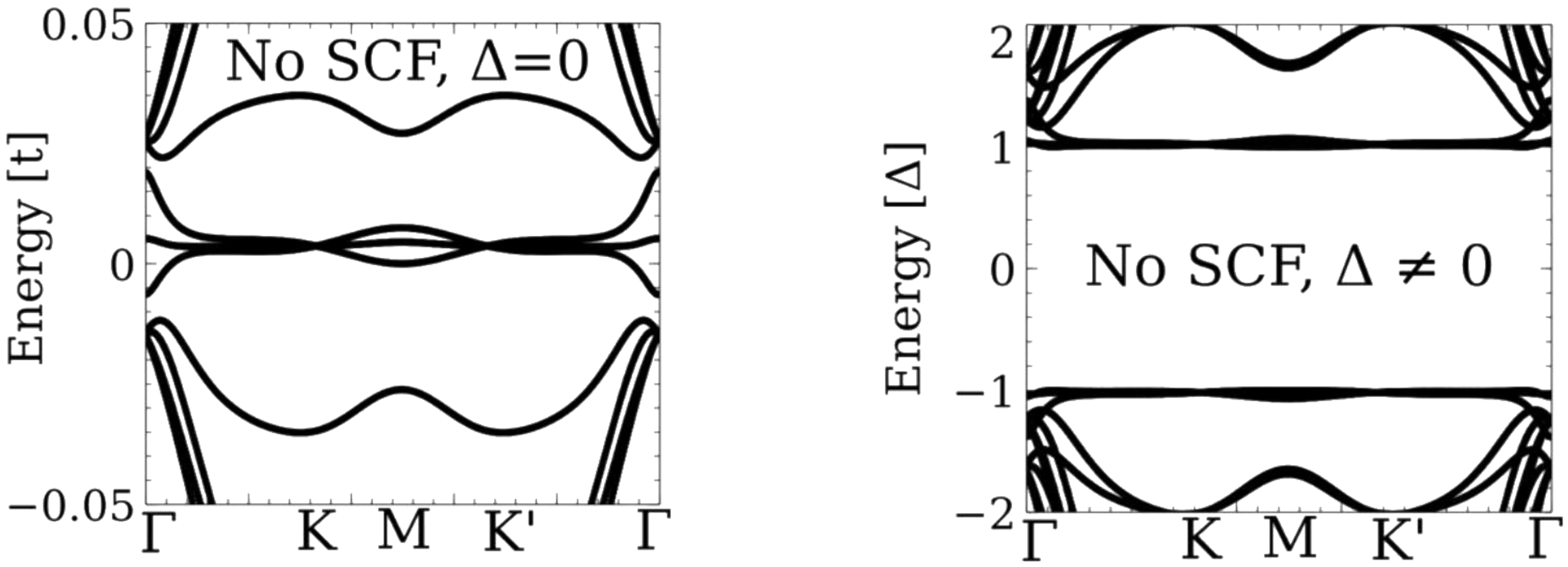

s-wave superconductivity opens up a gap in the electronic spectra

Electronic structure including repulsive interactions

With interaction-induced magnetism

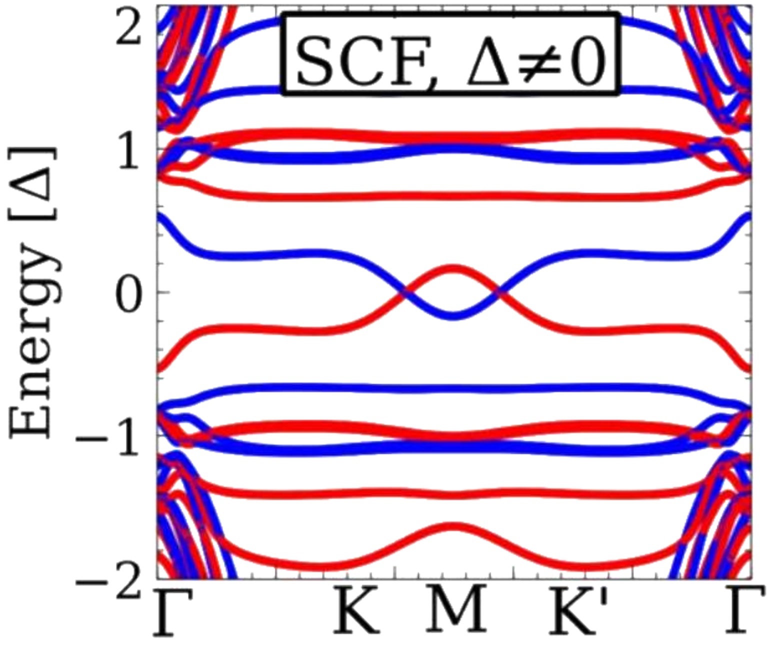

Without interaction-induced magnetism

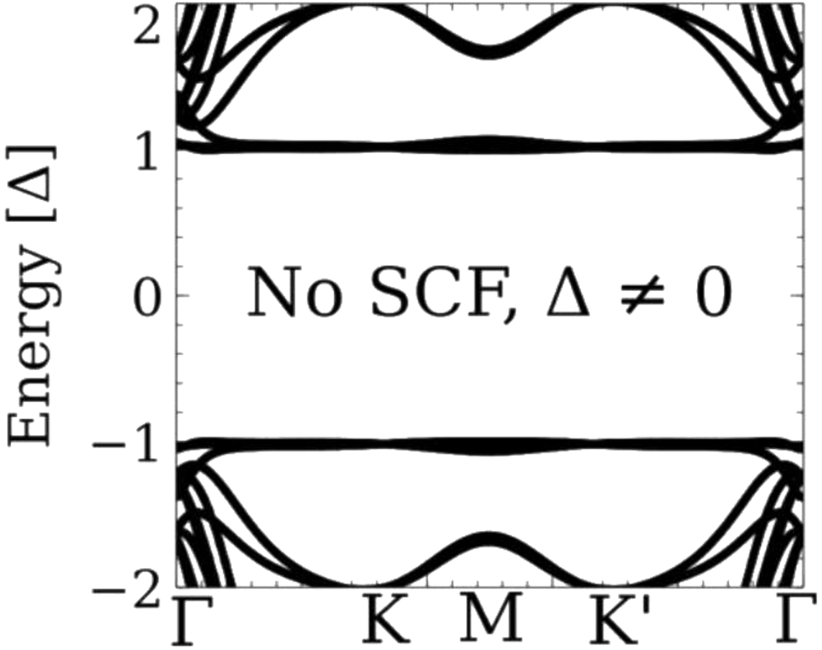

Impurity-induced magnetism and s-wave superconductivity gives rise to in-gap Yu-Shiba-Rusinov states

Electronic structure including repulsive interactions

With interaction-induced magnetism

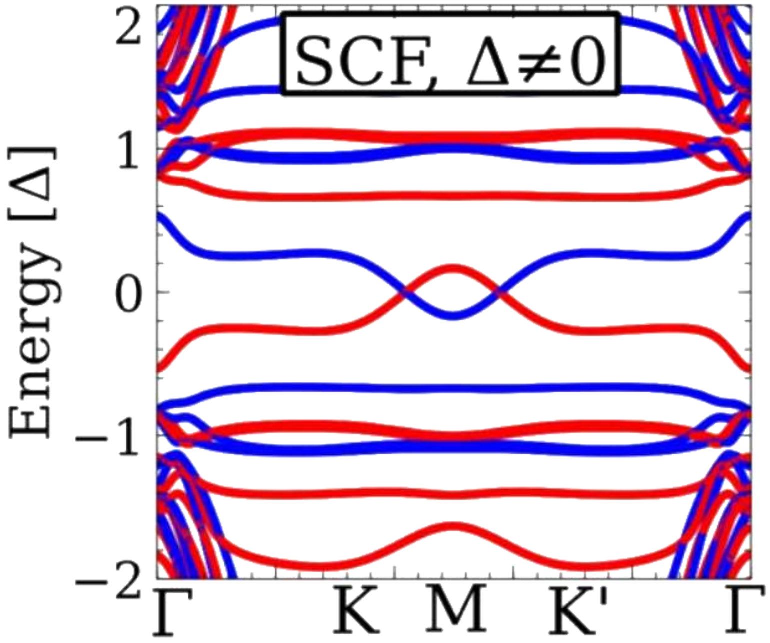

Spatial distribution of the in-gap YSR states

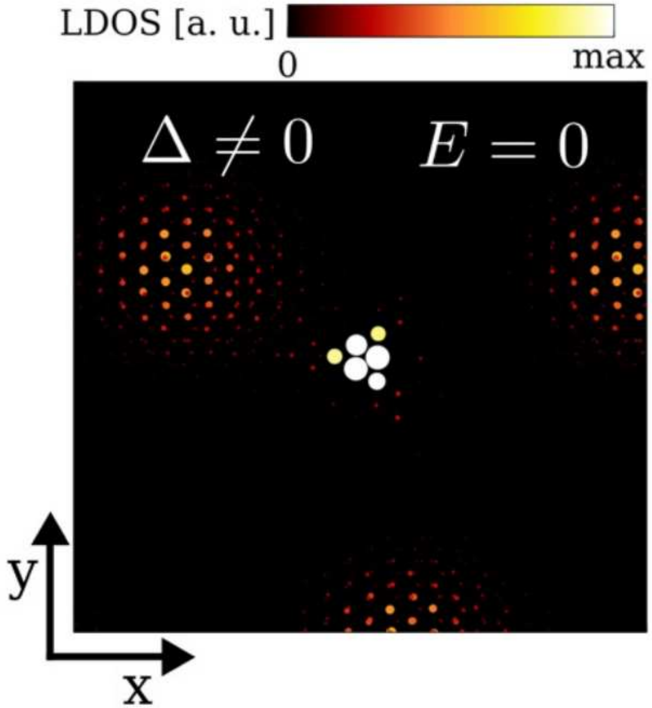

In-gap modes appear around the interaction-induced impurity magnetic moment

Impurities in twisted trilayer graphene

Structure of mirror-symmetric twisted graphene trilayer

Top view

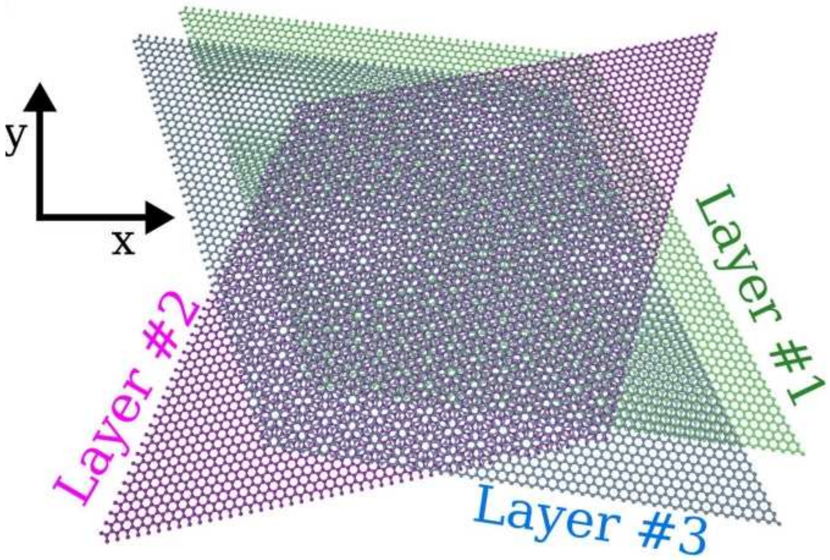

Lateral view

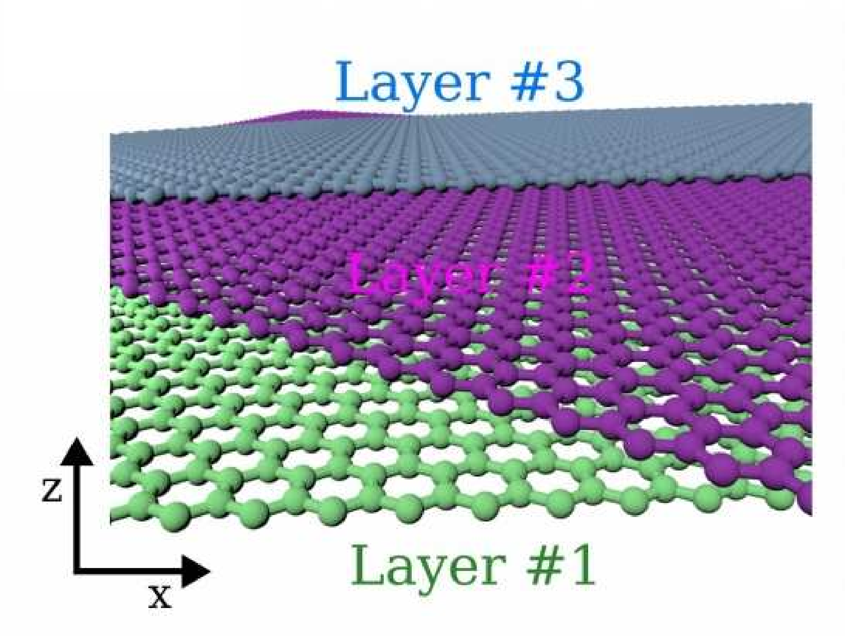

Electronic structure of twisted trilayer

Without an interlayer bias

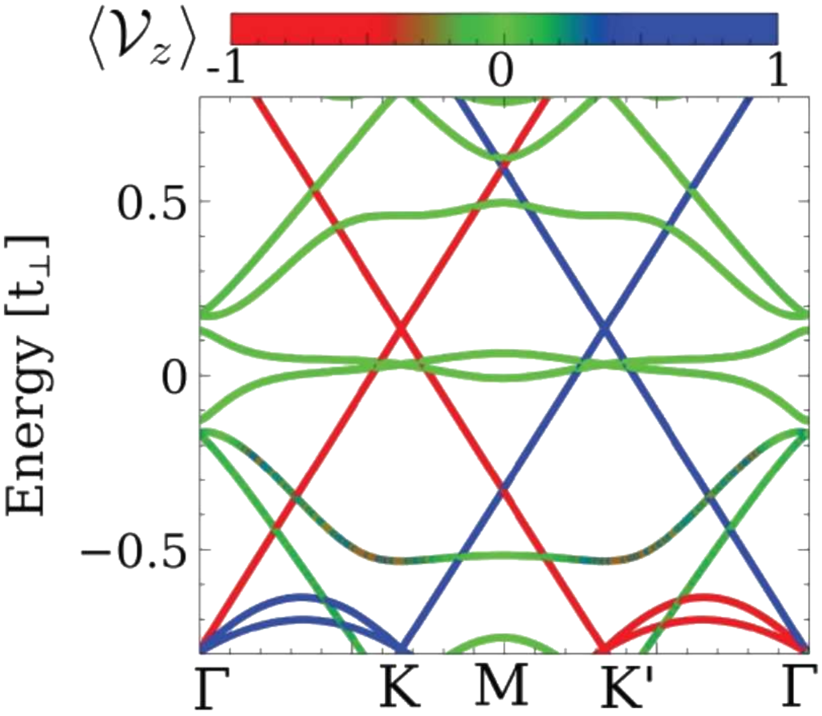

With an interlayer bias

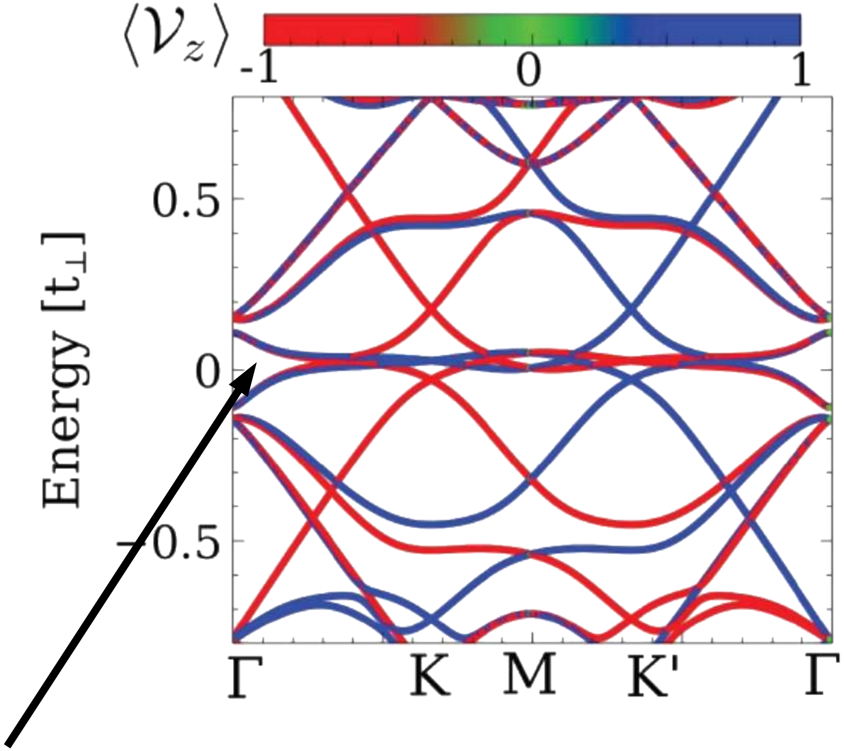

An interlayer bias creates internal topological valley currents

Internal topological valley currents in a twisted trilayer

The spatially resolved valley current is defined from the valley Chern number

$$C_V = C_K - C_{K'} = \int \chi_V(\mathbf{r}, \omega) d^2\mathbf{r}\, d\omega$$

Spatially and frequency resolved valley Chern density

$$\chi_V(\mathbf{r}, \omega)$$

It represents bulk valley currents

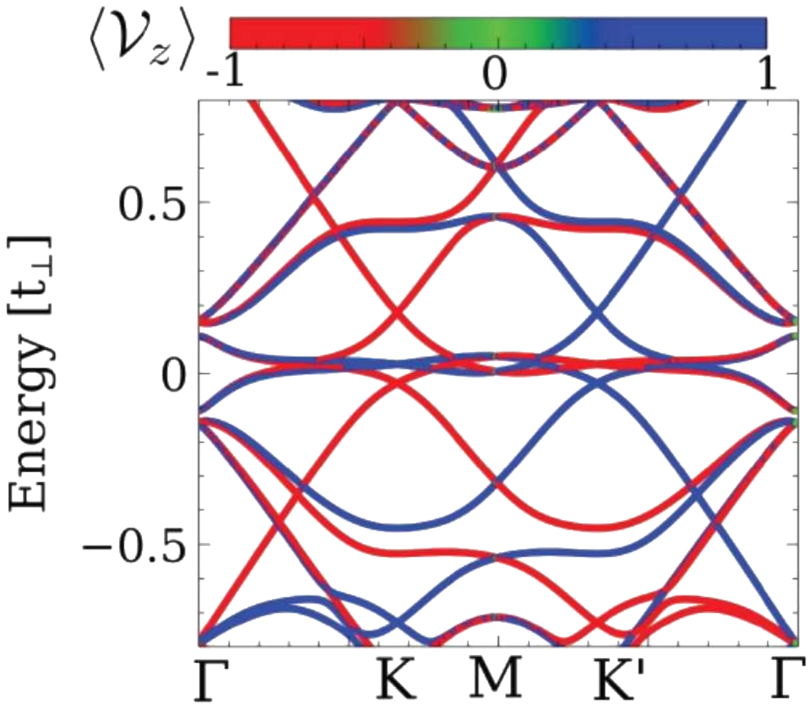

Internal topological valley currents in a twisted trilayer

Bulk valley current

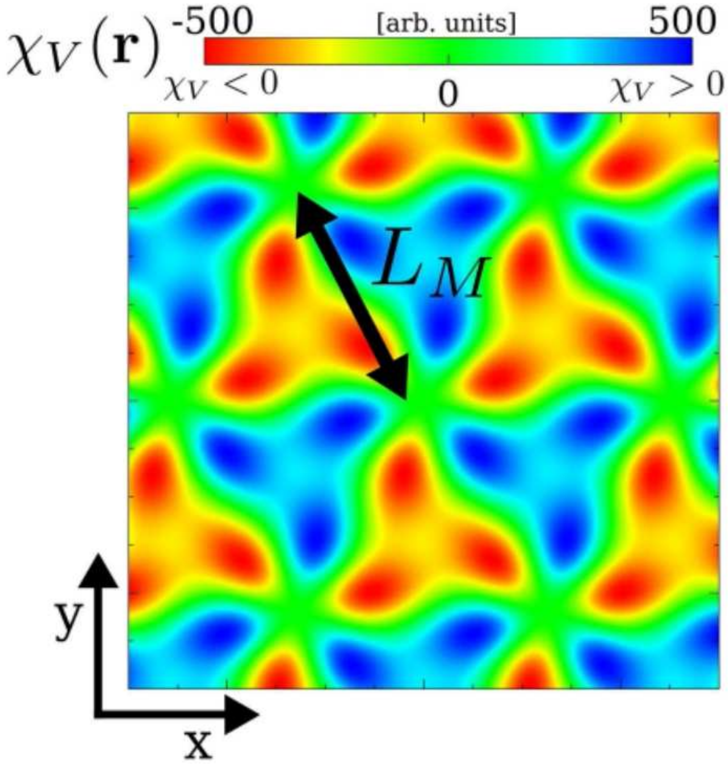

Band structure

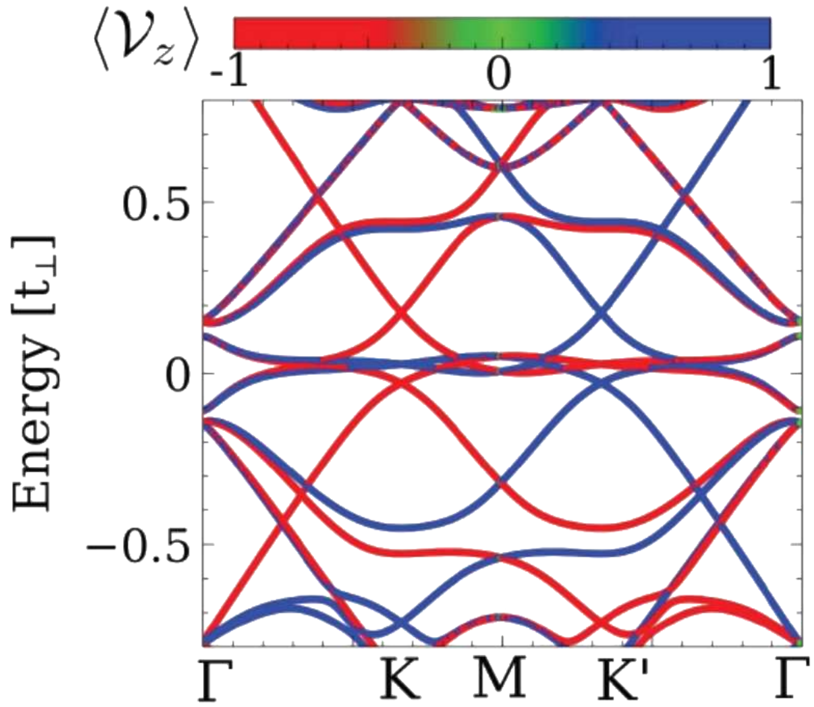

Internal topological valley currents emerge in the moire supercell

Weak impurity in a twisted graphene trilayer

Bulk valley current

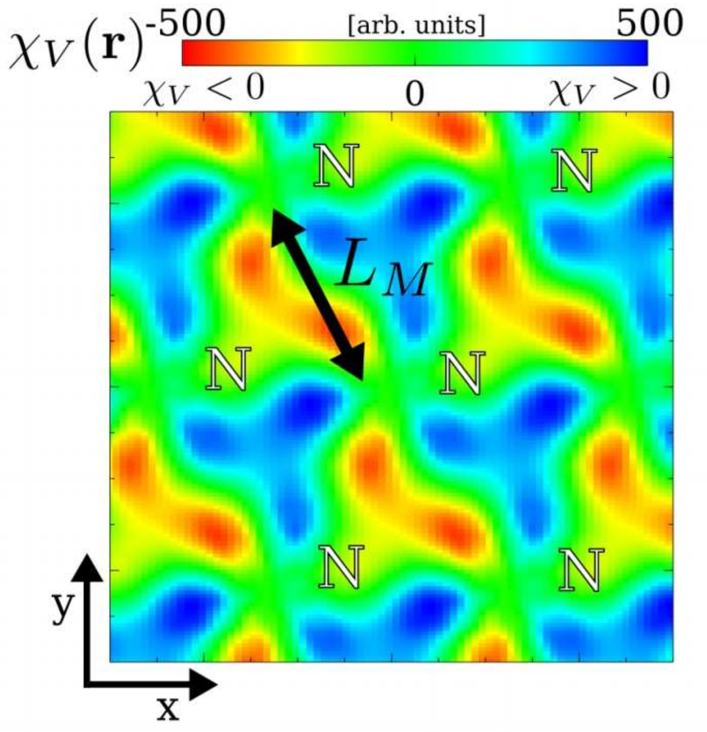

Band structure

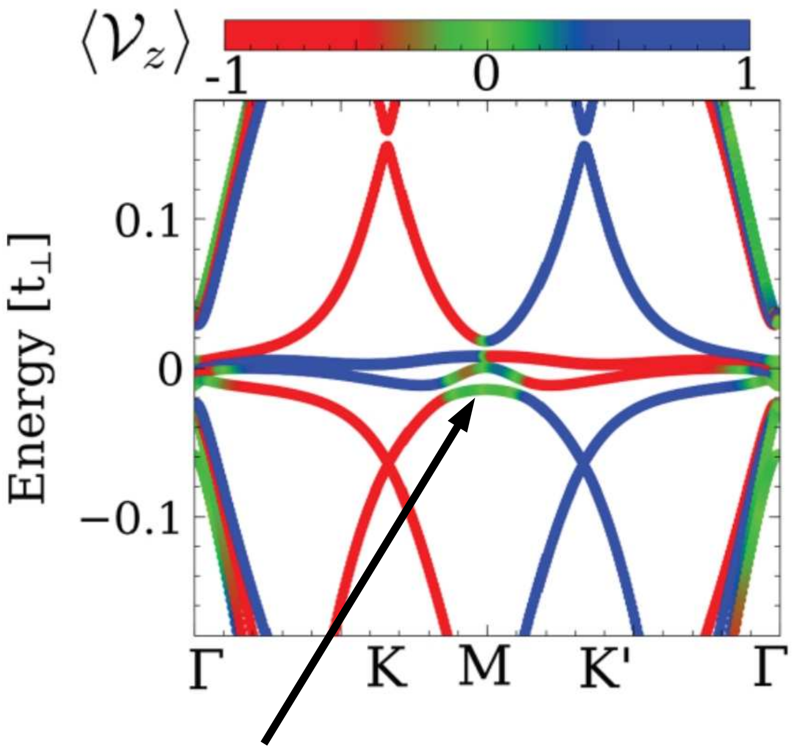

Weak impurities give rise to valley mixing at low energies

Disruption of valley currents by an impurity

Pristine

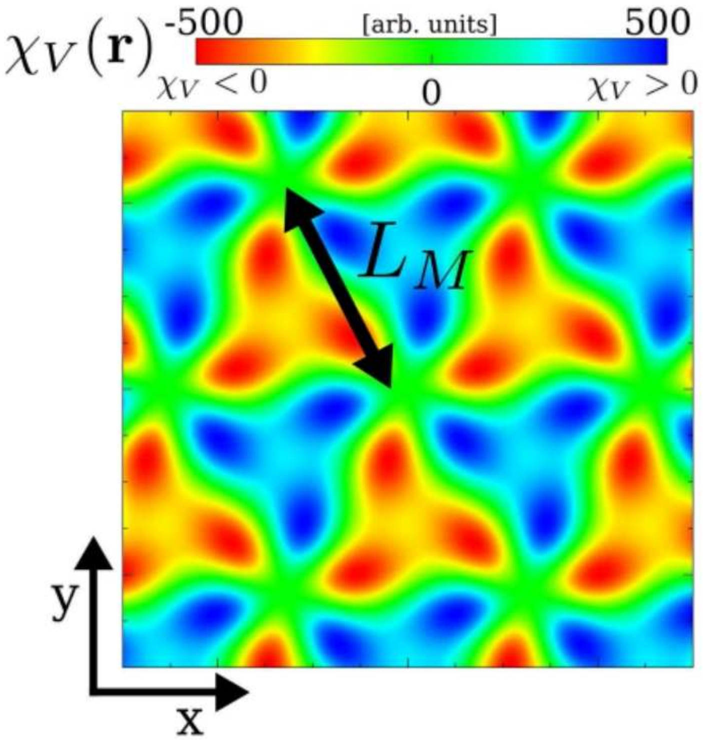

Weak impurity

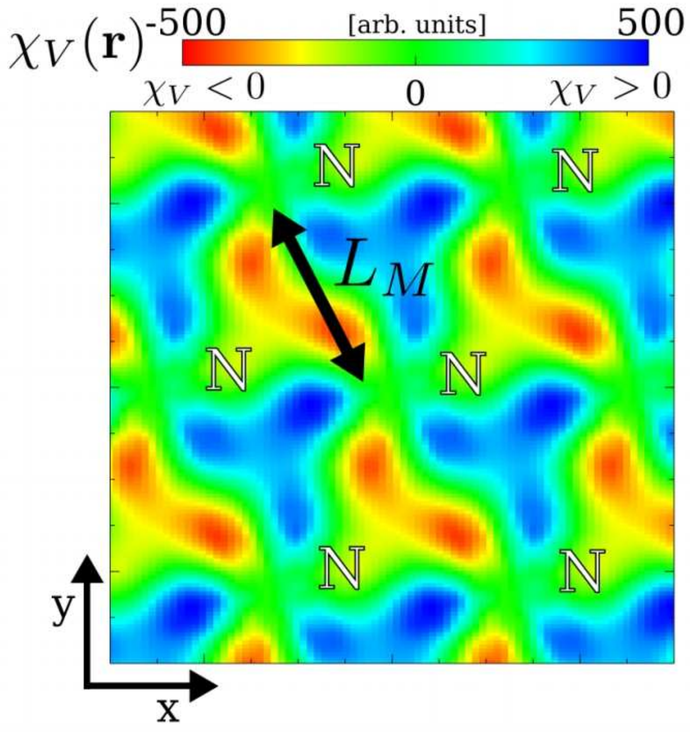

Weak impurities disrupt the valley currents in twisted graphene trilayers

Impurities in a twisted topological superconductor

Topological superconductivity in CrBr3/NbSe2 heterostructure

$CrBr_3/NbSe_2$ heterostructure

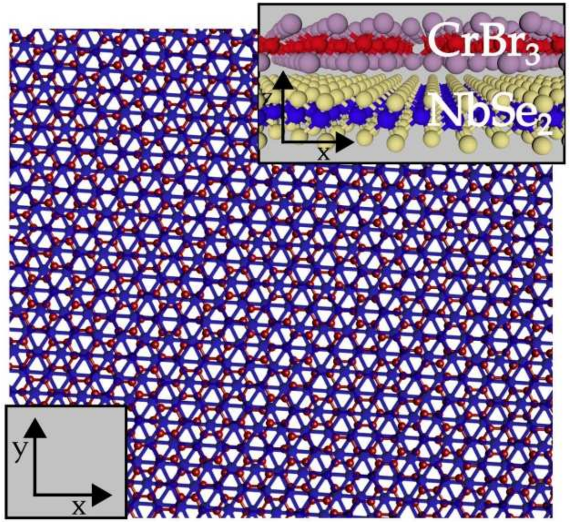

Nature 588, 424–428 (2020)
Nano Lett. 2022, 22, 1, 328–333

Zero bias dIdV

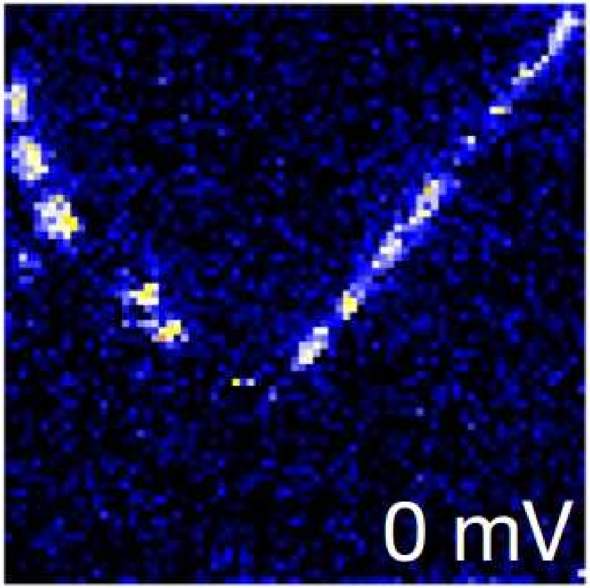

A topological superconducting state appears in $CrBr_3/NbSe_2$

$CrBr_3/NbSe_2$ heterostructure

Topography

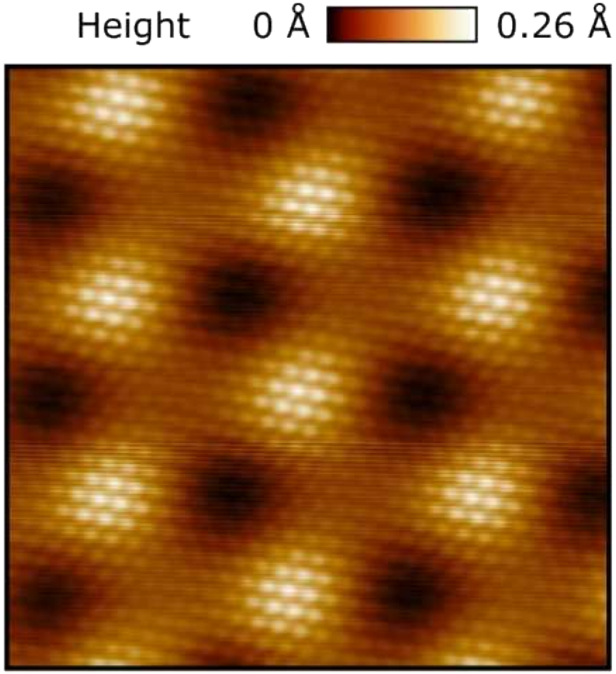

didV of the Yu-Shiba-Rusinov states

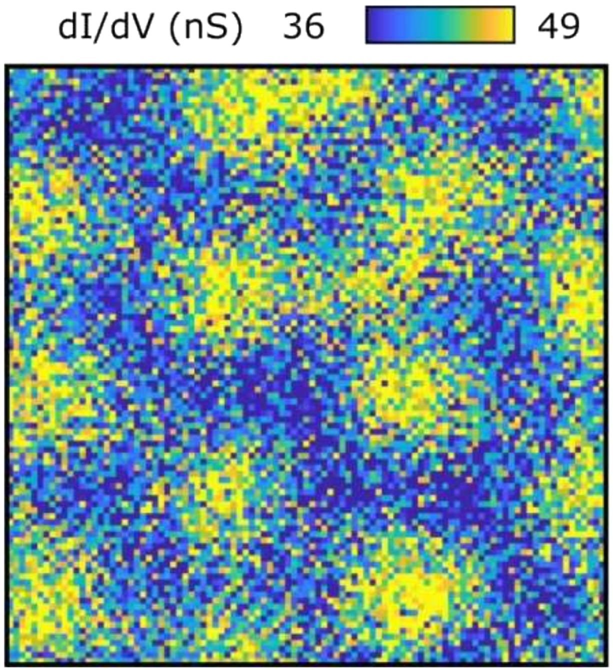

The low energy properties are affected by the moire pattern

Hamiltonian for the pristine moire topological superconductor

Structure

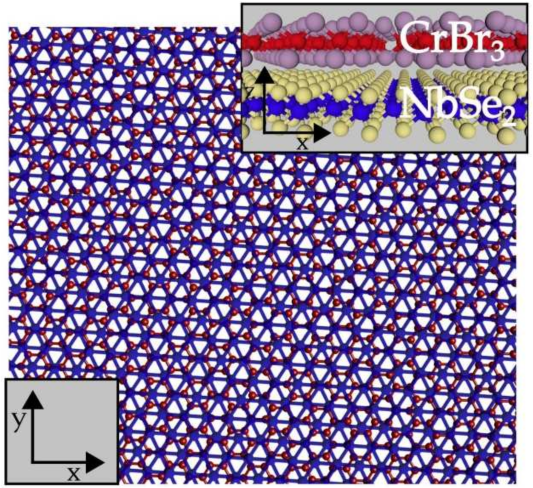

Exchange profile

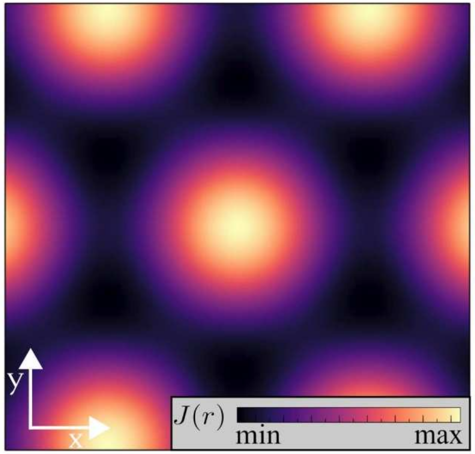

Superconducting profile

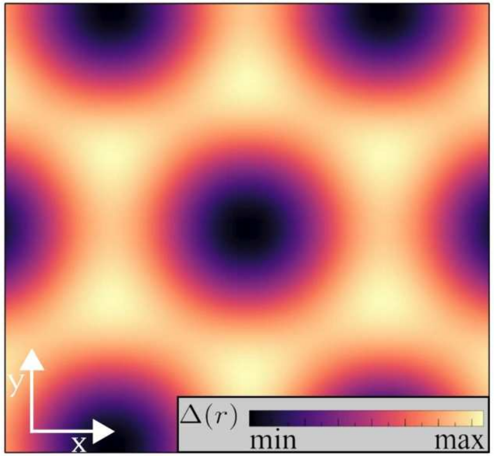

$$\mathcal{H}_0 = \mathcal{H}_{\text{kin}} + \mathcal{H}_J + \mathcal{H}_R + \mathcal{H}_{\text{SC}}$$

Kinetic energy

Exchange coupling

Rashba SOC

s-wave superconductivity

Hamiltonian for the defective moire topological superconductor

Full Hamiltonian

$$\mathcal{H} = \mathcal{H}_0 + \mathcal{H}_{\text{imp}}$$

Local impurity in the moire system

$$\mathcal{H}_{\text{imp}} = w \sum_s c^\dagger_{n,s} c_{n,s}$$

Weak impurity

$$w \to 0$$

Strong impurity

$$w \to \infty$$

$$\mathcal{H}_0 = \mathcal{H}_{\text{kin}} + \mathcal{H}_J + \mathcal{H}_R + \mathcal{H}_{\text{SC}}$$

Kinetic energy

Exchange coupling

Rashba SOC

s-wave superconductivity

Impurities in the moire topological superconductor

Band structure in the absence of impurity

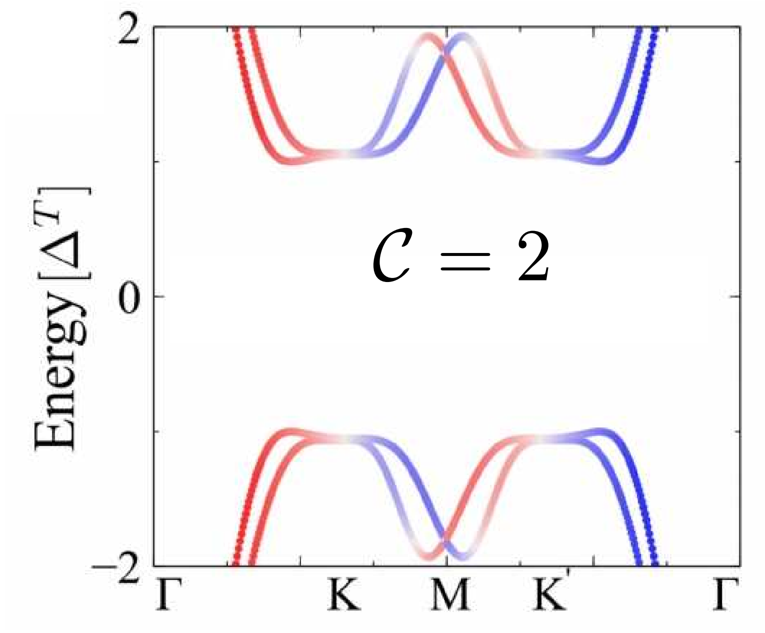

Band structure in the presence of an impurity

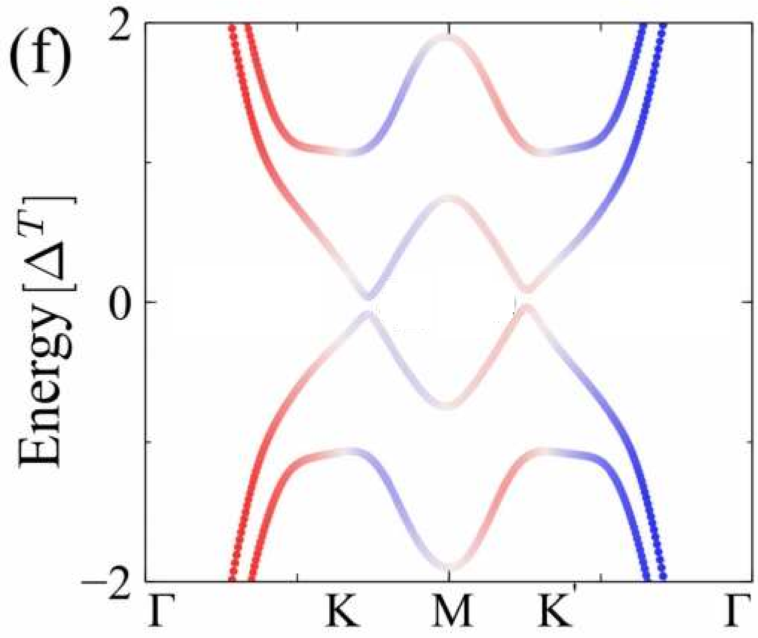

Strong local impurities decrease the size of a topological gap

Gap as a function of the location of a strong impurity

Gap as function of the location of the impurity

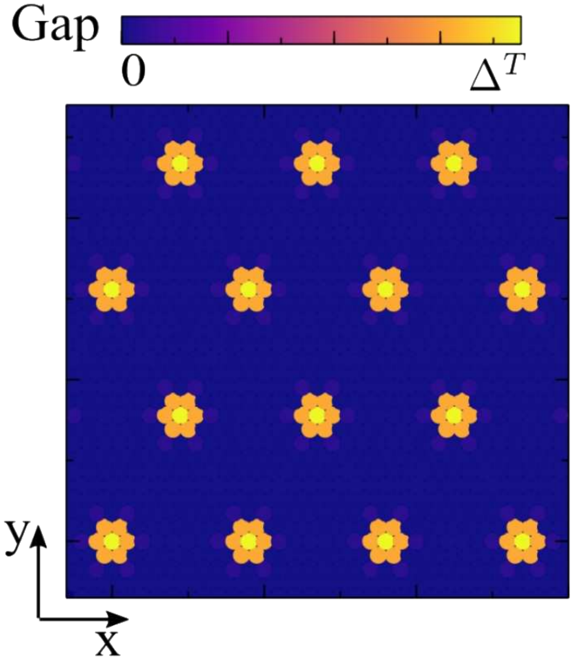

Band structure for impurity at the center

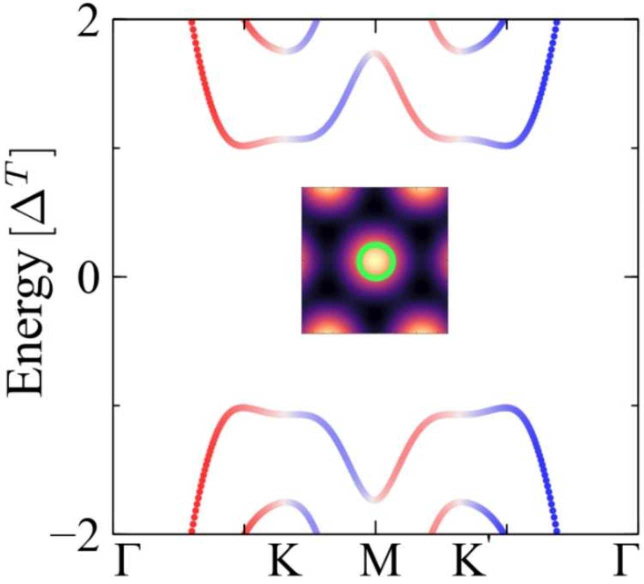

Band structure for impurity away from the center

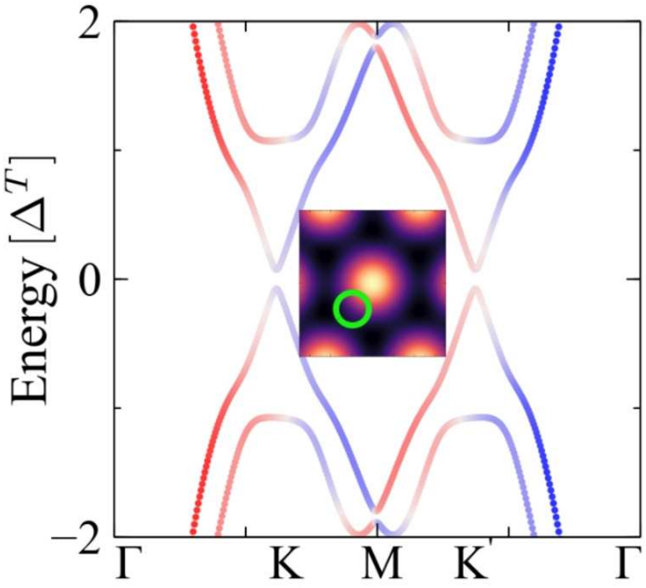

The location of the impurity strongly affects the resulting gap

Gap as a function of the location of a strong impurity

Gap as function of the location of the impurity

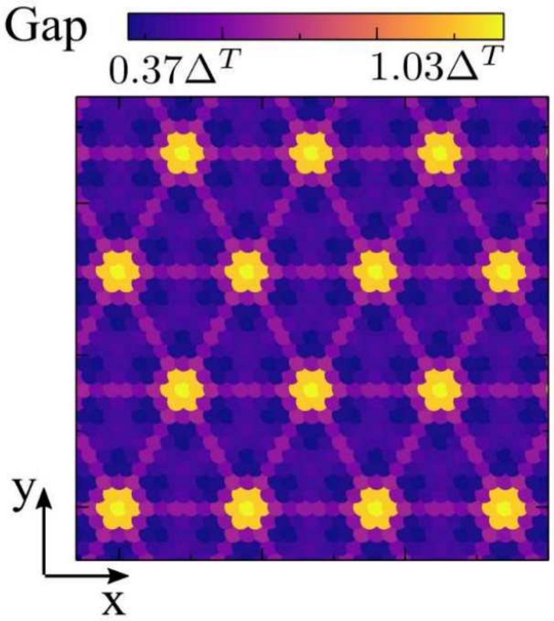

Band structure for impurity at the center

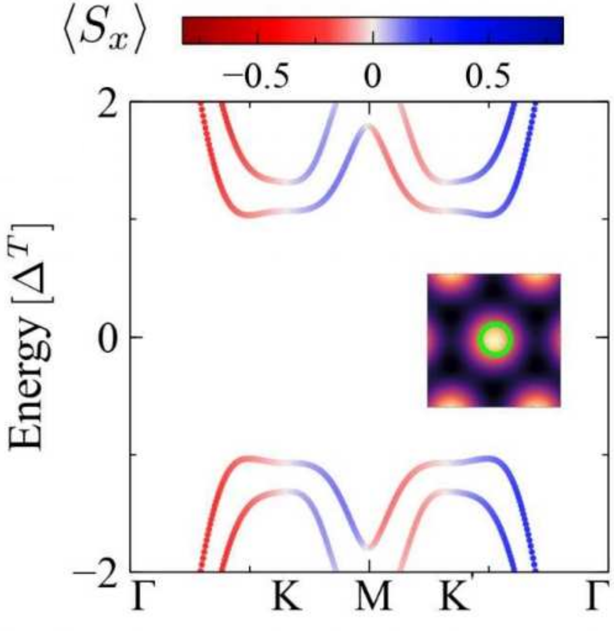

Band structure for impurity away from the center

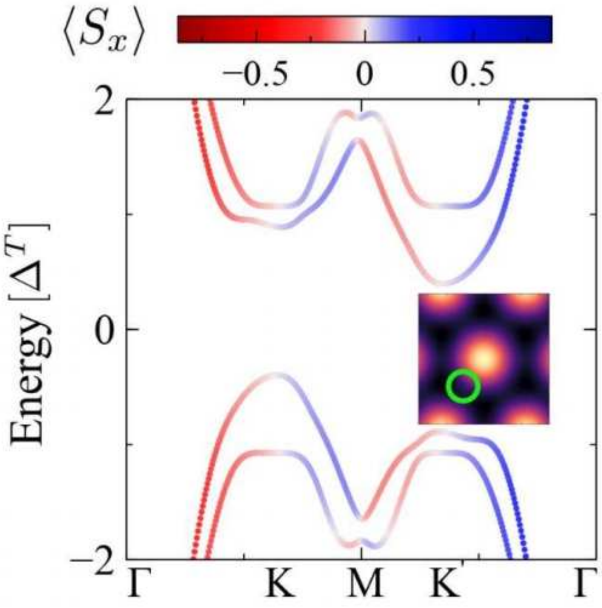

The location of the impurity strongly affects the resulting gap

Gap as function of location for different moire unit cells

11x11 supercell

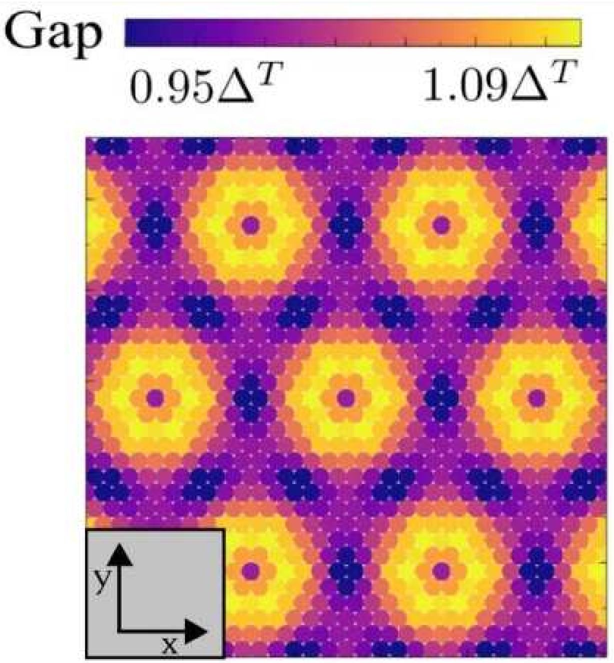

15x15 supercell

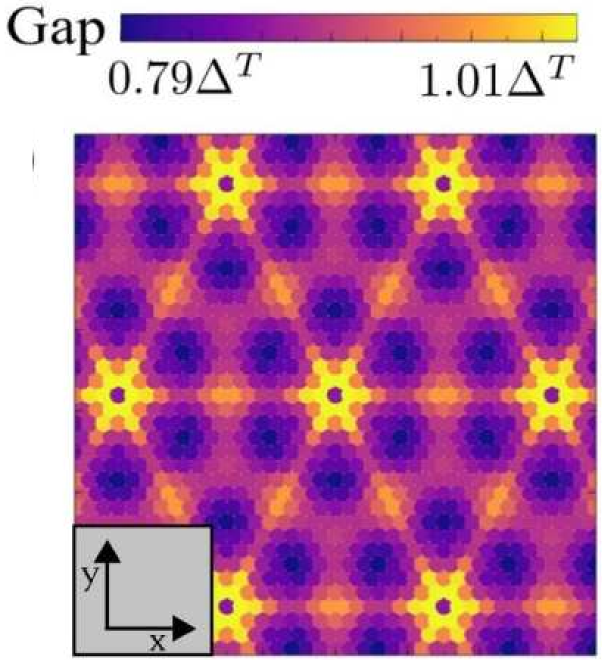

17x17 supercell

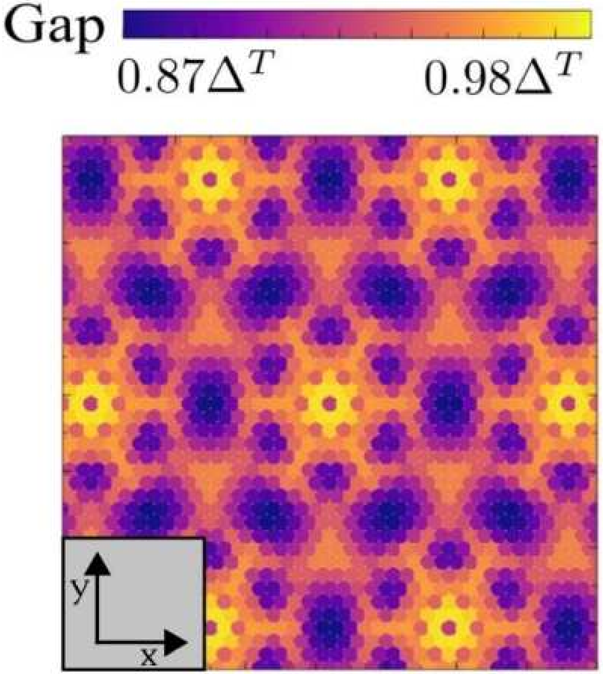

Detrimental locations for impurities depend on the specific moire supercell

The single impurity limit

We now look at the single impurity regime

From the Green's function, we can compute the spatially resolved density of states at the energy of the YSR state

$$\rho(\mathbf{x},\omega) = -\frac{1}{\pi}\sum_{s,\tau}\langle \mathbf{x}, s, \tau|\mathrm{Im}(G_V(\omega))|\mathbf{x}, s, \tau\rangle$$

Dyson equation for a single impurity

$$G_V(\omega) = [\omega - H_V - \Sigma(\omega) + i0^+]^{-1}$$

Selfenergy from the pristine regime

$$G_0(\omega) = [\omega - H_0 - \Sigma(\omega) + i0^+]^{-1}$$

YSR without moire

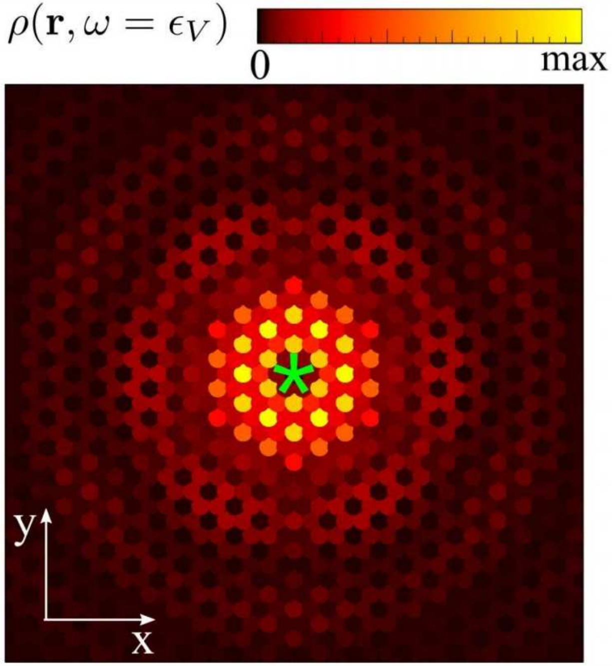

Single impurity in a topological moire superconductor

Wavefunction of the YSR state for different impurity locations

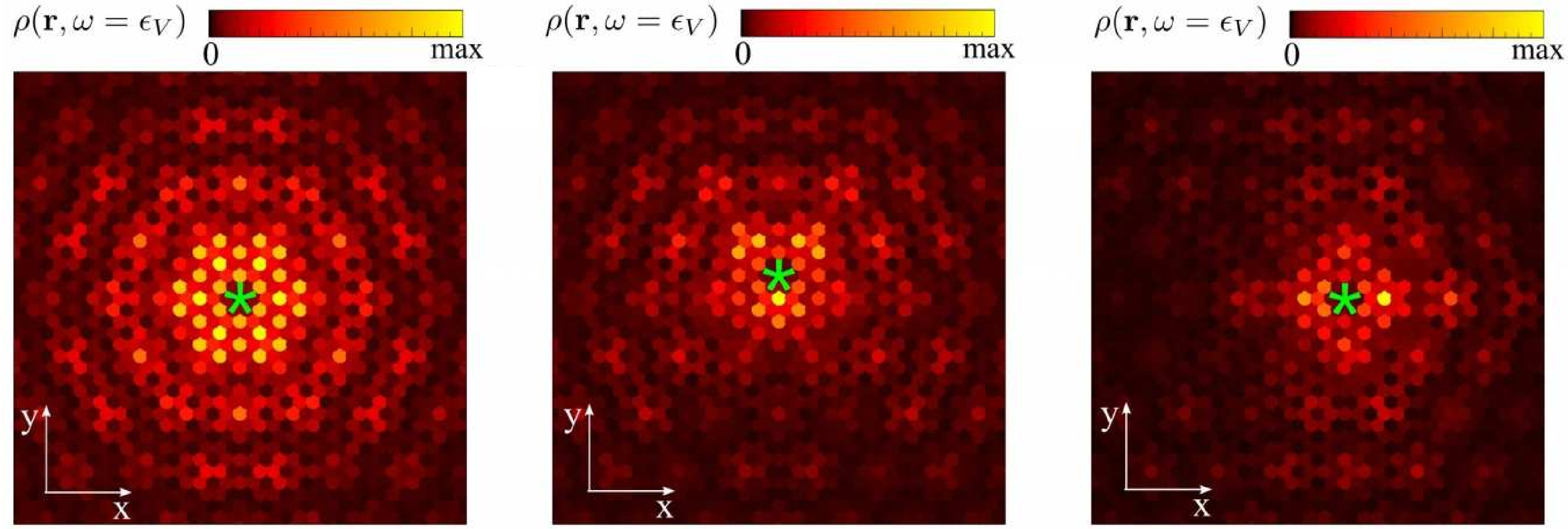

The YSR state wavefunction and the moire give rise to interference effects

Computing electronic properties

Quantum Lattice: A user interface to compute electronic properties

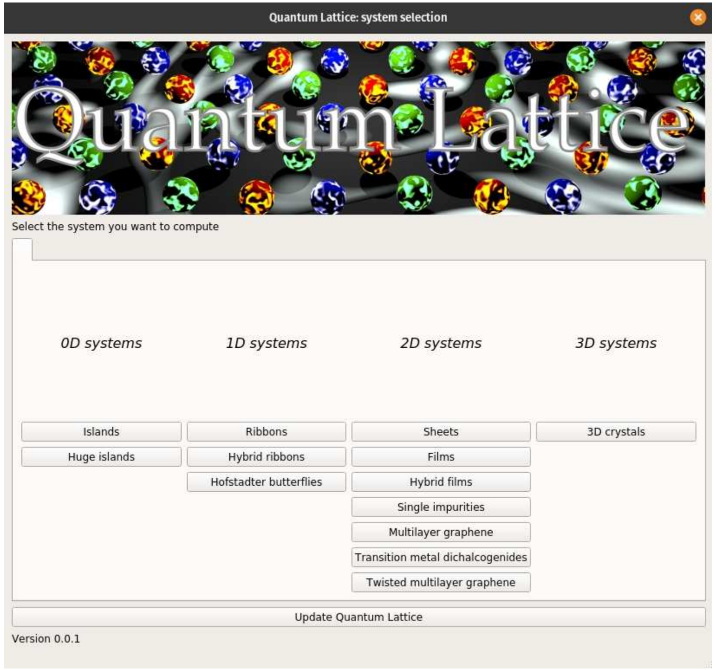

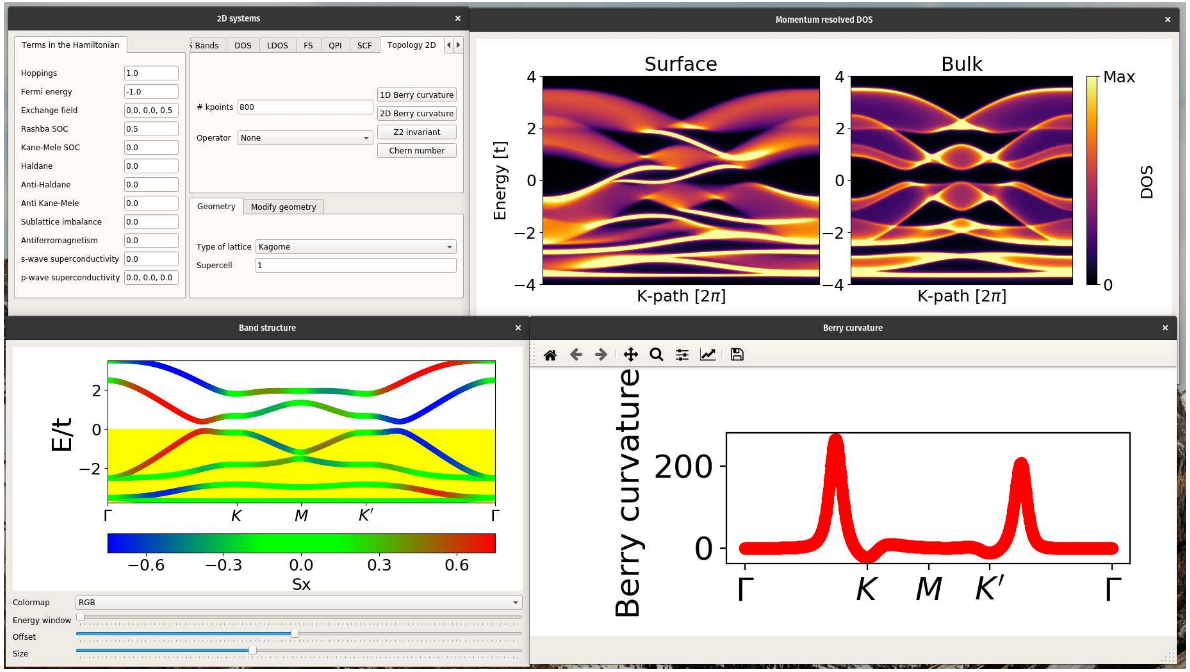

Quantum Lattice: open source interactive interface for tight binding modeling

https://github.com/joselado/quantum-lattice

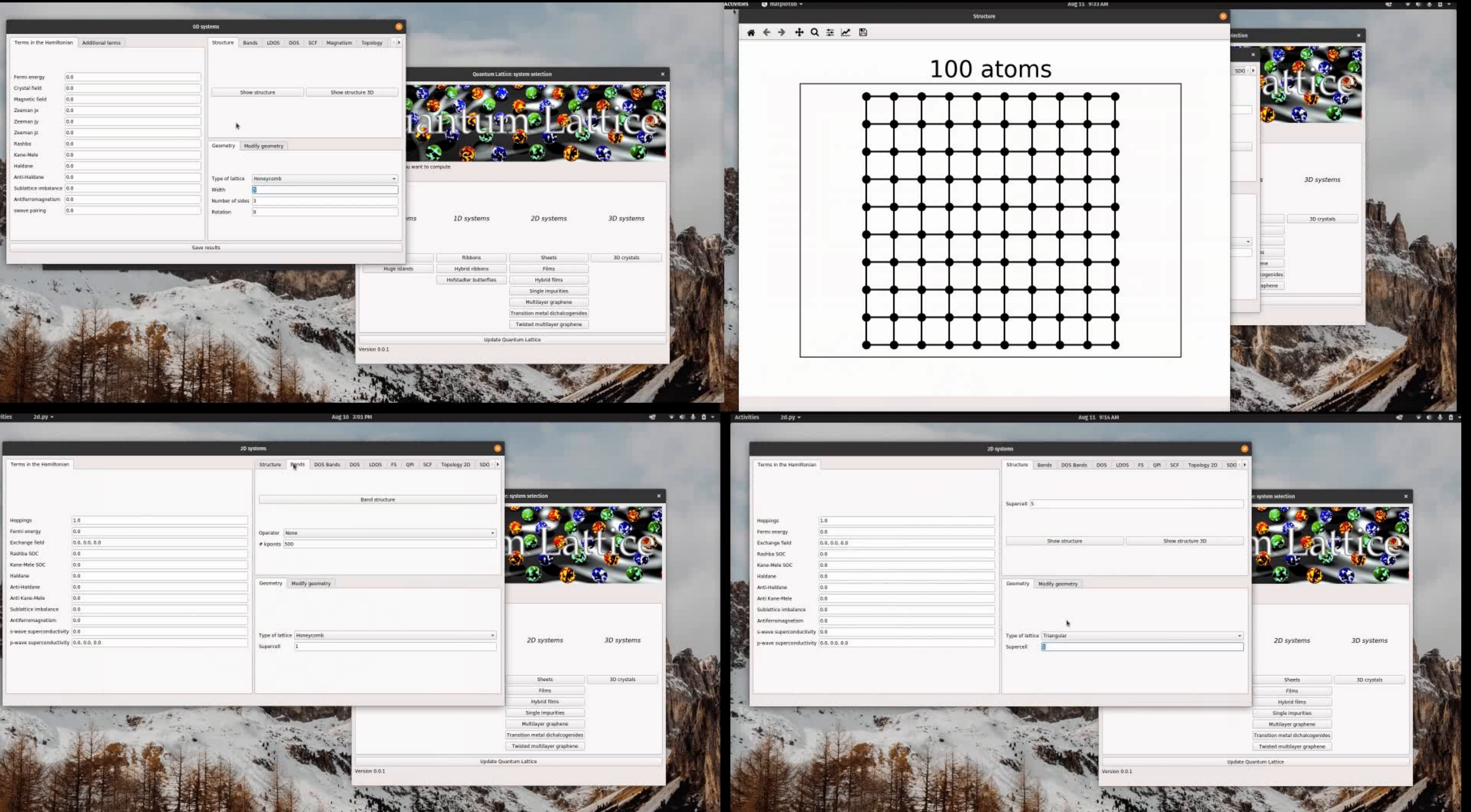

0D systems
Terms in the Hamiltonian
Additional terms
Structure
Bands
LDOS
DOS
SCF
Magnetism
Topology
Fermi energy 0.0
Crystal field 0.0
Magnetic field 0.0
Zeeman jx 0.0
Zeeman jy 0.0
Zeeman jz 0.0
Rashba 0.0
Kane-Mele 0.0
Haldane 0.0
Anti-Haldane 0.0
Sublattice imbalance 0.0
Antiferromagnetism 0.0
swave pairing 0.0
Show structure
Show structure 3D
Geometry
Modify geometry
Type of lattice Honeycomb
Width
Number of sides 3
Rotation 0
Save results
Quantum Lattice: system selection
1D systems
2D systems
3D systems
Ribbons
Sheets
3D crystals
Huge islands
Hybrid ribbons
Films
Hofstadter butterflies
Hybrid films
Single impurities
Multilayer graphene
Transition metal dichalcogenides
Twisted multilayer graphene
Update Quantum Lattice
Version 0.0.1
Structure
100 atoms
2D systems
Terms in the Hamiltonian
Structure
Bands
DOS Bands
DOS
LDOS
FS
QPI
SCF
Topology 2D
SDO
Band structure
Operator None
kpoints 500
Hoppings 1.0
Fermi energy 0.0
Exchange field 0.0, 0.0, 0.0
Rashba SOC 0.0
Kane-Mele SOC 0.0
Haldane 0.0
Anti-Haldane 0.0
Anti Kane-Mele 0.0
Sublattice imbalance 0.0
Antiferromagnetism 0.0
s-wave superconductivity 0.0
p-wave superconductivity 0.0, 0.0, 0.0
Geometry
Modify geometry
Type of lattice Honeycomb
Supercell 1
Supercell 5
Show structure
Show structure 3D
Type of lattice Triangular

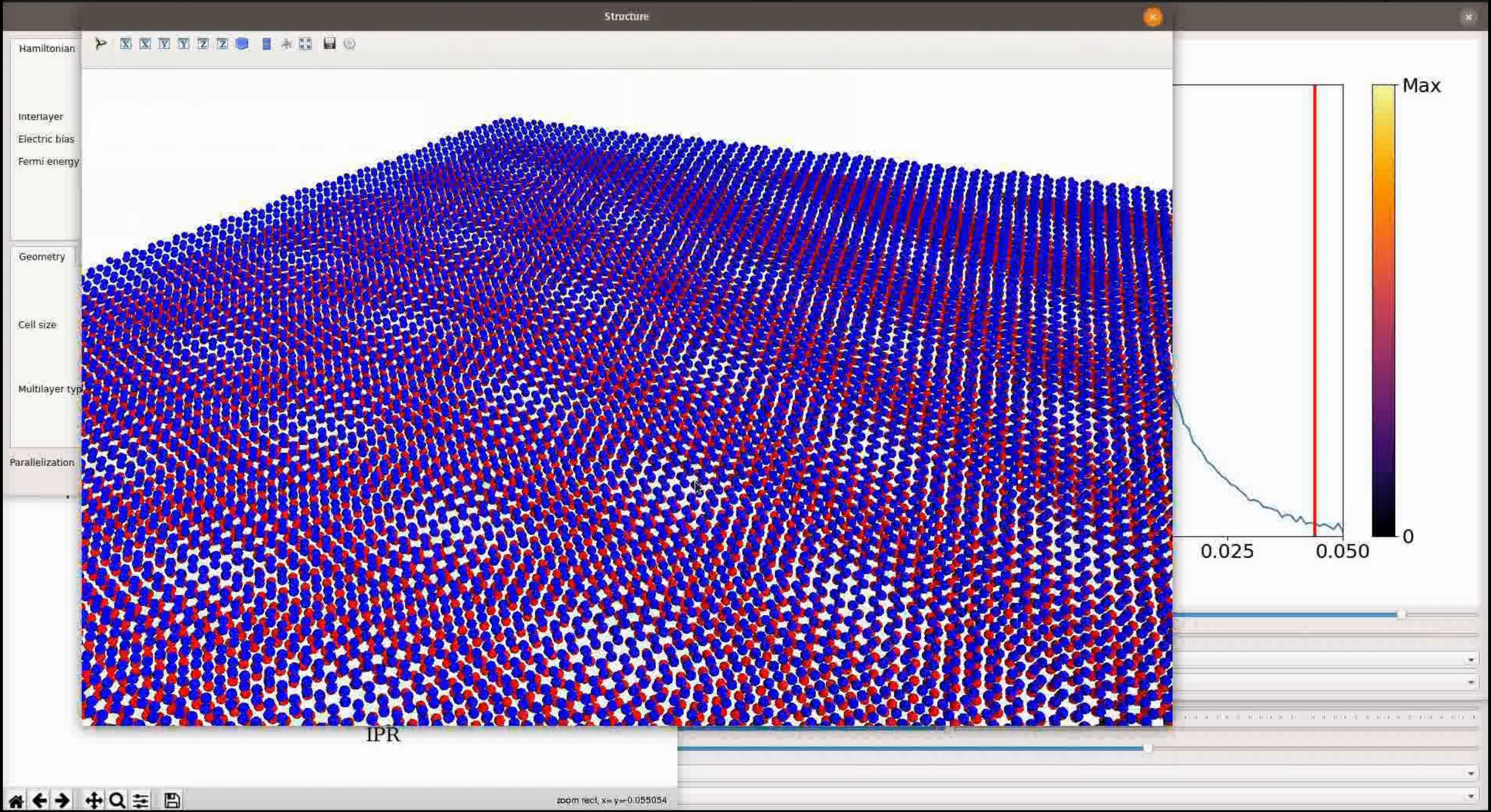
Structure
Hamiltonian
Interlayer
Electric bias
Fermi energy
Geometry
Cell size
Multilayer typ
Parallelization
Max
0
0.025
0.050
IPR
zoom rect, x=y=0.055054

Take home

Impurities in twisted moire systems can have strong impacts in the low energy dispersion, creating resonant states and affecting topological and correlated states

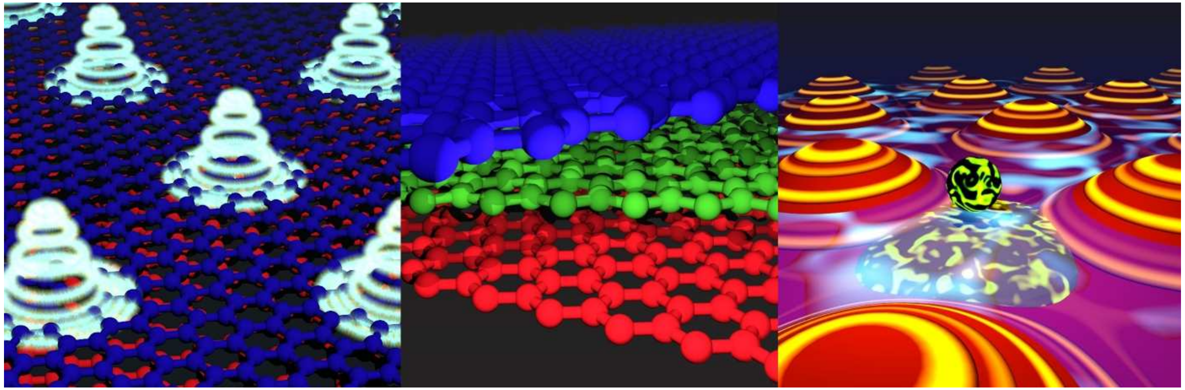

Thank you!

Funding from

J&AE JANE AND AATOS ERKKO FOUNDATION

SUOMEN AKATEMIA

Phys. Rev. B 99, 245118 (2019)
Phys. Rev. Materials 3, 084003 (2019)
Phys. Rev. Research 2, 033357 (2020)
arXiv:2202.11003 (2022)